Enterococcal Metabolite Cues Facilitate Interspecies Niche Modulation and Polymicrobial Infection

Damien Keogh[1,2], Wei Hong Tay[1,2], Yao Yong Ho[1,2], Jennifer L. Dale[6], Siyi Chen[4], Shivshankar Umashankar[3], Rohan B. H. Williams[3], Swaine L. Chen[4,5], Gary M. Dunny[6] and Kimberly A. Kline[1,2]*

[1]Singapore Centre for Environmental Life Science Engineering, Nanyang Technological University, 60 Nanyang Drive, Singapore 637551

[2]School of Biological Sciences, Nanyang Technological University, 60 Nanyang Drive, Singapore 637551

[3]Singapore Centre for Environmental Life Science Engineering, National University of Singapore, 28 Medical Drive, Singapore, 114756

[4]National University of Singapore, Yong Loo Lin School of Medicine, Department of Medicine, Division of Infectious Diseases, 1E Kent Ridge Road, NUHS Tower Block, Level 10, Singapore 119074

[5]Genome Institute of Singapore, GERMS and Infectious Disease Group, 60 Biopolis Street, Genome, #02-01, Singapore 138672

[6]Department of Microbiology, University of Minnesota Medical School, Minneapolis, Minnesota, USA

*Correspondence: kkline@ntu.edu.sg

Summary

Enterococcus faecalis is frequently associated with polymicrobial infections of the urinary tract, indwelling catheters, and surgical wound sites. *E. faecalis* co-exist with *Escherichia coli* and other pathogens in wound infections but mechanisms that govern polymicrobial colonization and pathogenesis are poorly defined. During infection, bacteria must overcome multiple host defenses, including nutrient iron limitation, to persist and cause disease. In this study, we investigated the

contribution of *E. faecalis* to mixed species infection when iron availability is restricted. We show that *E. faecalis* significantly augments *E. coli* biofilm growth and survival *in vitro* and *in vivo* by exporting L-ornithine, which *E. coli* utilizes for enhanced biofilm growth. This metabolic cue facilitates *E. coli* biosynthesis of the enterobactin siderophore to overcome iron-limiting conditions that otherwise restrict its growth. Thus, *E. faecalis* modulates its local environment by contributing growth-promoting cues that allow co-infecting organisms to overcome iron limitation and promotes interspecies infections.

Keywords

Polymicrobial infection, iron, nutritional immunity, *Enterococcus faecalis*, *Escherichia coli*, wound infection

Introduction

Polymicrobial infections account for approximately 25% of all bacterial infections, the majority of which are biofilm-associated (Magill et al., 2014). Biofilm associated infections have increased antibiotic tolerance and are often chronic in nature, contributing to many of the most prevalent and difficult to treat nosocomial infections. Chief among these are surgical site, wound, and catheter-associated urinary tract infections (CAUTI) (Klevens et al., 2007). Wound infections are often polymicrobial, where *Pseudomonas aeruginosa, Staphylococcus aureus, Escherichia coli,* and *Enterococcus faecalis* are frequent constituents (Bowler et al., 2001, Dowd et al., 2008, Gjodsbol et al., 2006).

E. faecalis is a common member of intestinal microbiota of humans (Lebreton et al., 2014). Enterococci are also opportunistic pathogens associated with endocarditis, surgical site and other wound infections, urinary tract infection, and CAUTI (Maki and Tambyah, 2001, Nallapareddy et al., 2006, Nielsen et al., 2013, Dowd et al., 2008). *E. faecalis* is associated with 11% of all CAUTI, often as part of a polymicrobial community that frequently includes *E. coli* (Flores-Mireles et al., 2015).

Enterococci are associated with more than 5% of surgical site infections (Giacometti et al., 2000) and up to 35% of wounds in diabetic individuals (Citron et al., 2007).

E. faecalis is nutritionally fastidious and requires environments that provide nutrients that it does not biosynthesize independently (Lebreton et al., 2014). Despite this, *E. faecalis* is remarkably tolerant of iron limited environments and has been shown to grow *in vitro* in medium where iron is almost absent; a characteristic of some lactic acid bacteria where manganese serves as a substitute cofactor essential in many cellular enzymes (Bruyneel et al., 1989, Marcelis et al., 1978, Weinberg, 1997, Archibald, 1986). Iron acquisition systems, such as transporters for siderophores or iron from heme-iron sources have been extensively characterized in *E. coli* and other bacterial pathogens, have not been functionally characterized in *E. faecalis* (Budzikiewicz, 2010, Miethke and Marahiel, 2007, Neilands, 1993, Neilands, 1995). Metabolic compounds with broad metal chelation specificity have been detected in *E. faecalis*; however no structural determination of these compounds or functional characterization of systems involved in their export or uptake has been performed (Lisiecki and Mikucki, 2006, Lisiecki and Mikucki, 2004). Transcriptomic studies highlight putative transport systems with homology to siderophore systems; however roles for these putative systems in iron uptake functionality have not been examined (Vebo et al., 2009, Vebo et al., 2010). The importance of iron for the polymicrobial community, and the ability of *E. faecalis* to thrive in low-iron environments, suggest that *E. faecalis* may be successful in polymicrobial interactions when iron is limiting.

In this study, we show that *E. faecalis* promotes the growth and survival of *E. coli* biofilm when iron is limited. In a mouse model of wound infection, *E. coli* CFU are significantly increased during co-infection with *E. faecalis* compared to single species infections. Using *in vitro* models of iron restricted growth, we demonstrate that *E. faecalis* specifically augments *E. coli* growth and survival in biofilms, and not planktonic growth. We show that *E. coli* enterobactin siderophore production is necessary for augmented growth during co-infection with *E. faecalis*. Ornithine exported by *E.*

faecalis serves as a cue to promote *E. coli* biofilm. This work demonstrates how *E. faecalis* alters the local environment to promote polymicrobial infections by modulating the amino acid pool available to *E. coli* and thereby shifting metabolism in favor of siderophore biosynthesis.

Results

***E. faecalis* promotes the growth of *E. coli* biofilms under iron limitation**

Iron limitation is an effective host innate defense during bacterial infection (Ganz and Nemeth, 2012). Therefore we established *in vitro* assays that mimic this environment for the study of polymicrobial interactions. Using macrocolonies as a surrogate for biofilm formation, we determined the effects of iron limitation on the growth of *E. faecalis* and *E. coli* biofilm (**Figure 1A,D,E**). Growth limitation of *E. coli* macrocolonies occurred at 0.1mM of the iron chelator 2,2'-dipyridyl (22D) onwards whereas *E. faecalis* macrocolony growth remained unaffected at both 0.1mM and 0.7mM 22D and was not visibly affected at concentrations as high as 2.0mM 22D (**Figure 1C,F,G**), consistent with reports that other lactic acid bacteria can tolerate low iron concentrations (Imbert and Blondeau, 1998, Weinberg, 1997, Bruyneel et al., 1989). We also observed higher *E. faecalis* tolerance to iron limitation, compared to *E. coli*, in planktonic culture (**Figure S1A,B**).

To investigate the effects of iron limitation on mixed species biofilm growth, we grew macrocolonies at varying inoculation ratios, keeping the total number of bacteria in the starting inoculum constant. We observed restricted biomass accumulation for the mixed 1_{Ec}:1_{Ef} macrocolonies at 0.1mM 22D, similar to single species *E. coli* macrocolonies (**Figure 1A**). However, increasing the ratio of *E. faecalis* to *E. coli* to 1_{Ec}:19_{Ef} gave rise to augmented biomass compared to the 1_{Ec}:1_{Ef} macrocolony and compared to single species macrocolonies (**Figure 1B**). We therefore focused on the 1_{Ec}:19_{Ef} inoculum ratio for the remainder of our *in vitro* studies. Addition of ferric chloride to 22D-chelated media restored *E. coli* macrocolony size to that of the mixed 1_{Ec}:19_{Ef} macrocolony (**Figure 1C**) and similar to *E. coli* colonies grown in the absence of 22D (**Figure 1A**) showing that mixed species biomass augmentation is specific to iron-limitation.

To evaluate the growth kinetics of *E. coli* and *E. faecalis* in single and mixed species macrocolonies, we enumerated the colony forming units (CFU) in colonies at 24, 72 and 120 hours under both iron replete conditions and with 0.1mM and 0.7mM 22D. The presence of *E. faecalis* resulted in significantly more *E. coli* in the mixed species macrocolony with 0.1mM 22D at 120hr (**Figure 1D**). This growth effect was more pronounced at higher chelator concentrations where higher *E. coli* CFU were observed in mixed species colonies as early as 72hr. In contrast, *E. faecalis* CFU were similar between both single and mixed species macrocolonies (**Figure 1E**). Growth of *E. faecalis* was lower in mixed species macrocolonies at 72hr and 120hr under 0mM or 0.1mM 22D (**Fig E**), when *E. coli* is still growing well, suggesting that the differences in *E. faecalis* growth could be due to nutrient competition arising from robust *E. coli* growth (**Figure 1D**).

To determine whether enhanced *E. coli* growth in the presence of *E. faecalis* was specific to macrocolonies, we examined planktonic growth as well as a static biofilm assays using polystyrene microtiter plates and quantification via crystal violet as a standard assay for investigation of biofilm formation (O'Toole, 2011). When supplemented with 0.1mM 22D and incubated under the same conditions as that of the macrocolony assays, we observed that biofilm biomass was significantly greater for mixed species biofilms than that of single species biofilm (**Figure 1F**). *E. faecalis* mediated enhancement of *E. coli* growth did not occur in planktonic culture (**Figure 1G**). Therefore, *E. faecalis* augmentation of *E. coli* growth is a biofilm specific phenotype.

A soluble, diffusible *E. faecalis* factor promotes *E. coli* biofilm growth

To investigate whether *E. faecalis* promotes *E. coli* growth in biofilms in a contact-dependent manner, we inoculated the *E. coli* and *E. faecalis* macrocolonies at increasing distances from one another. In this proximity assay, *E. coli* macrocolonies were larger at closer distances (1cm) to *E. faecalis* macrocolonies than at greater distances (5cm) (**Figure 2A**). Increased *E. coli* colony size correlated with higher *E. coli* CFU at 120hr (**Figure 2B**), suggesting that enhanced macrocolony size was dependent on a soluble, diffusible factor that required 120hr to reach *E. coli* and the for the growth phenotype to become apparent.

E. faecalis proximity promotes differential *E. coli* gene expression

To interrogate the mechanism governing *E. faecalis*-mediated growth promotion of *E. coli* under iron limitation, we surveyed the transcriptomes of both *E. coli* and *E. faecalis* macrocolonies in the proximity assay using RNA-Seq (see **Supplemental Experimental Procedures**). We predicted that the transcriptome of *E. coli* would be significantly different between the proximal and distal colonies due to differences in growth and physiology. In contrast, since *E. faecalis* CFU at proximal and distal sites were unchanged, we predicted only modest differences in the transcriptome between the two colony locations. We further hypothesized that additional changes in *E. coli* mRNA levels would be specifically related to *E. faecalis*-mediated enhanced growth under the iron limited conditions of the proximity assay. Consistent with our predictions, only 5% (122 genes) of *E. faecalis* genes were differentially regulated (≥2-fold change, FDR<0.05) when grown close to *E. coli*, whereas 51% (2617 genes) of *E. coli* genes were significantly changed in their expression levels when in close proximity to *E. faecalis*. We then determined whether genes that are members of known biochemical pathways, as defined by KEGG (Kanehisa et al., 2010, Kanehisa et al., 2014), were present in the set of *E. coli* genes showing higher overall expression in macrocolonies closer to *E. faecalis* than compared to those more distal, at a proportion greater than random expectation (see **Experimental Procedures**). From this statistical enrichment analysis, we observed pathways related to growth and metabolism within the top 100 differentially regulated genes attain statistical significance (Benjamini-Hochberg adjusted $P<0.05$) (**Figure 2C, Table S2,3**). KEGG classification and manual curation of all differentially regulated genes enabled examination of expression for individual genes within each pathway (**Figure 2D**). These findings supported that genes related to growth and metabolism constituted the bulk of expression changes and showed that of the 18 *E. coli* genes increased in expression by LogFC≥5.0 between the distal and proximal *E. coli* sites, 7 were members of the *biosynthesis of siderophore group non-ribosomal peptides* pathway (KO01053) specifically functioning in yersiniabactin biosynthesis (**Figure 2E**). Genes encoding components of the membrane transport and biosynthesis systems for the enterobactin (*fepABD*, *entABDEF* and *fes*) and

salmochelin (*iroEN*) siderophores displayed increased expression with log fold-change values ranging from 1 to 3. The salmochelin glucosyltransferase *iroB* was notably the only siderophore associated gene downregulated at LogFC -1.39. Of the two ferrous iron uptake systems (FeoAB and EfeUOB) only *efeUOB* displayed increased expression. All iron storage and assimilation genes identified had increased expression with log fold-change values ranging from 1 to 2. Of the 6 genes detected encoding systems for xenosiderophore uptake, 5 of these were decreased in expression by LogFC≤-1. Interestingly, and in contrast to *E. coli, E. faecalis* genes with homology to characterized systems involved in iron utilization were expressed at lower levels in close proximity to *E. coli*. This suggests that these systems in *E. faecalis* may function in a manner different to that of other characterized bacterial iron acquisition systems since iron is limiting and likely to be further restricted due to the abundance and proximity of *E. coli* iron scavenging systems (**Figure 2F**).

***E. coli* ferrous uptake systems do not contribute to *E. faecalis* driven *E. coli* growth promotion**

The two *E. coli* ferrous iron uptake systems, encoded by *feoAB* and *efeUOB*, were downregulated and upregulated respectively in proximity to *E. faecalis*. These systems are both regulated in response to iron availability, and *efeUOB* can be induced under acidic conditions (Cao et al., 2007, Miethke et al., 2013). Since *E. faecalis* is a lactic acid-producing bacterium, we hypothesized that local acidification could affect iron solubility and potentially induce the *E. coli efeUOB* ferrous iron uptake genes. Overlaying macrocolonies in the proximity assay at 7hr, 48hr and post-72hr with a pH indicator solution demonstrated that local pH changes occur, with *E. coli* macrocolonies being in the acidic range (approximately pH5.5) at 7hr and 48hr (**Figure S1C**). To determine the role of the ferrous systems in mediating *E. coli* growth enhancement, we constructed in-frame deletion mutants of the permease components of each system, *feoB* and *efeU,* individually and together. However, these mutants were not attenuated for *E. faecalis*-enhanced *E. coli* growth in the proximity assay indicating that *E. coli* mechanisms responding to *E. faecalis* proximity do not involve ferrous iron acquisition (**Figure S1D**).

Enterobactin siderophore production is essential for *E. faecalis* promotion of *E. coli* growth

E. coli strain UTI89 used in this study encodes three siderophore biosynthetic operons, responsible for yersiniabactin, enterobactin, and salmochelin which are essential for colonization and virulence in multiple models of infection (Hancock et al., 2008, Wiles et al., 2008, Chaturvedi et al., 2012, Henderson et al., 2009, Lv and Henderson, 2011, Garcia et al., 2011). The siderophore systems in *E. coli* were more highly transcribed in close proximity to *E. faecalis* at 120hr, with the virulence associated siderophore yersiniabactin being the most highly expressed. Enterobactin, which is common to most *E. coli* strains, and its glucosylated derivative salmochelin, were also significantly upregulated (Raymond et al., 2003, Hantke et al., 2003). Using previously characterized mutants for each siderophore alone and in combination (Lv et al., 2014, Henderson et al., 2009), we found that a Δ*entB* mutant that is unable to produce enterobactin does not exhibit enhanced growth in close proximity to *E. faecalis* (**Figure 3A,D).** In contrast, salmochelin and yersiniabactin were dispensable for *E. faecalis* mediated *E. coli* growth enhancement (**Figure 3B,C)**. Macrocolony CFU for each of these mutants cultured independently was equivalent to wild type *E. coli* (**Figure S1E**). Therefore, enterobactin production specifically, and not that of the other siderophores, was essential for *E. faecalis* mediated enhancement of *E. coli* growth under iron limitation.

Co-infection with *E. faecalis* augments *E. coli* virulence in a mouse model of wound infection

E. faecalis is frequently co-isolated from wound infections with *E. coli* and other pathogens (Browne et al., 2001, Neut et al., 2011). To evaluate the impact of *E. faecalis* on *E. coli* within polymicrobial infections, we used a modified mouse wound excisional model (Dalton et al., 2011), and observed significantly more *E. coli* CFU from mixed species infections at 24 hours post infection (hpi) than in single species *E. coli* infections (**Figure 4A**). This recapitulates *in vitro* biofilm assay data showing that under iron limitation and when *E. coli* is present in lower abundance than *E. faecalis*, *E. faecalis* can promote the growth of *E. coli* biofilm (**Figure 1B,D,E,F & Figure 2A,B**). In comparison, the bacterial burden for *E. faecalis* from these mixed infections remained constant between single and mixed infections (**data not shown**). However, when the *E. coli* enterobactin mutant (Δ*entB*) was co-infected

with *E. faecalis* in the mouse wound excisional model, the *E. coli* Δ*entB* CFU from mixed species infections at 24hpi did not increase to the levels of wild type *E. coli* co-infected with *E. faecalis* (**Figure 4B**). The proportion of mixed species infections giving rise to high titer infections, above $1x10^5$CFU/wound, for *E. coli* wild type was 50-69% and for *E. coli* Δ*entB* was 15% (**Figure 4A,B**), indicating that the enterobactin mutant was unable to respond to *E. faecalis*–mediated augmentation in these infections. However, *E. coli* Δ*entB* CFU from single infections were comparable to those of single infections with wild type *E. coli* (**data not shown**). *E. faecalis* CFU from wounds co-infected with wild type *E. coli* and *E. coli* Δ*entB* at 24hpi were also the same (**Figure 4C**). Together, these data demonstrate that the *in vitro* biofilm assays mimic the *in vivo* infection environment and have identified conditions that alter infection outcome *in vivo*.

E. faecalis amino acid flux contributes to *E. coli* growth promotion

Transcriptional profiling of *E. faecalis* grown in close proximity to *E. coli* did not yield insights into the mechanism by which *E. faecalis* augments *E. coli* biofilm growth. Therefore, we screened an *E. faecalis* mariner transposon library (Kristich et al., 2008) for *E. faecalis* mutants that did not augment mixed species biofilm formation as measured by crystal violet staining (**Figure 1F**) (see **Supplemental Experimental Procedures**). We hypothesized that we would identify transposon mutants required to produce or export a signal that would ultimately impact enterobactin production in *E. coli*. We performed a primary screen for transposon mutants that gave rise to a 50% reduction in mixed species biomass in the presence of 0.1mM 22D, representing a defect in augmented growth (**Figure S2A**). Initial hits from the primary screen were revalidated, and mutants were selected in which mixed species biofilm biomass was significantly lower than that of the wild type mixed species biomass. **Table S4** lists the mutants identified following primary validation which can be divided into three classes: 1) transposon insertions in genes previously shown to contribute to *E. faecalis* single species biofilm formation in iron-replete media (Hancock and Perego, 2004, Nakayama et al., 2006, Pillai et al., 2004, Kristich et al., 2008, Gao et al., 2010, Bourgogne et al., 2006) 2) transposon

insertions in genes unique to this study, and 3) transposon insertions in intergenic regions. We excluded mutants defective for biofilm formation (class 1) from subsequent analyses, reasoning that general biofilm mutants would result in reduced mixed species biofilm due simply to fewer *E. faecalis* cells present in the assay. However, mutants unique to this study were likely to include insertion into *E. faecalis* genes important for biofilm formation in low iron environments, or into genes involved in signal production or signal exchange with *E. coli*. To differentiate between these possibilities, and to eliminate any mutants that had general growth defects, we performed single species planktonic and biofilm growth assays of *E. faecalis* transposon mutants in iron deplete and replete media. Transposon mutants with growth defects in either of these assays were also omitted from subsequent analysis. **Table 1** represents the final list of *E. faecalis* transposon mutants that formed single species biofilms as well as wild type but that did not augment *E. coli* growth and **Figure S2B** shows biofilm data for mixed species validation of these mutants. We performed whole genome sequencing to identify the insertion site for each mutant strain.

L-ornithine, but not branched chain amino acids, augments *E. coli* biofilm formation under iron limitation

The transposon library screen identified six genes that did not give rise to augmented mixed species biofilm biomass. We hypothesized that systems involved in signal production or mechanisms of signal exchange to *E. coli* would be governing the interaction of *E. faecalis* with *E. coli* resulting in growth augmentation. ArcD (OG1RF_10103) is the transporter responsible for importing L-arginine and simultaneously exporting L-ornithine as part of the arginine deiminase (ADI) pathway in *E. faecalis* (Barcelona-Andres et al., 2002). We therefore considered ArcD as a primary candidate since this was the only system facilitating export (L-ornithine) rather than import of a substrate and was therefore a strong candidate for signal exchange. To test this hypothesis, we performed single species *E. coli* biofilm assays under iron limited conditions and supplemented with L-ornithine in a concentration range up to 3.12mM. We observed significantly increased *E. coli* biofilm formation at

120hr at concentrations less than 1.5mM L-ornithine (**Figure 5A,B**). Biofilm growth inhibition occurs at concentrations greater than 1.5mM L-ornithine. In contrast, L-ornithine did not augment biofilm formation by the *E. coli* enterobactin mutant, suggesting that utilization of L-ornithine was linked to the biosynthesis of the enterobactin siderophore. We analyzed KEGG classification and manual curation data (**Figure 2D**) to determine if the *E. coli* uptake system for L-ornithine was differentially expressed when proximal to *E. faecalis.* The *argT hisJQMP* ABC transport system increases in expression with LogFC values of 2.521, 1.268 and 1.325 for *argT*, *hisM*, and *hisQ* respectively (Caldara et al., 2006).

Sequence homology and alignment analysis of the second transporter system (OG1RF_10187) from the transposon library screen predicted that putative substrates for this MFS symporter were branched chain amino acids. Symporters generally function by an inward-directed polarity facilitated by membrane potential; however, in the presence of the substrate on the *trans* side of the membrane this polarity can be reversed (Pao et al., 1998). We therefore supplemented *E. coli* biofilm assays with the branched chain amino acids valine, leucine and isoleucine and analyzed biofilm formation at 120hr. We did not observe increased biomass across a concentration range for any of these substrates (**Figure S2C**).

E. faecalis Constitutively Produces L-ornithine in Biofilm and *E. coli* Siderophore Production Increases Over Time

To verify that siderophores and L-ornithine are indeed present within the biofilm, we analyzed proximal and distal macrocolonies from the proximity assay at both 24hr and 120hr in an untargeted metabolomics survey (see **Supplemental Experimental Procedures**)**.** PCA plots were constructed for mass features detected by LC-MS based on proximity (**Figure S3A**) and time point (**Figure S3B**), compared to single species macrocolonies. This analysis shows that there are distinct global metabolite profiles between colonies from each species, and between the two sampling times. In addition, we detected the siderophores yersiniabactin (C12038) and vibriobactin (C06769) in all

samples but with greater abundance for yersiniabactin at 120hr in the proximity assay (**Figure S3C)**. Vibriobactin is not biosynthesized by *E. coli* UTI89. However, enterobactin and vibriobactin are both catecholate type siderophores and it is likely that enterobactin has been mis-identified from the KEGG database as vibriobactin. Consistent with RNA expression profiling, yersiniabactin is more abundant at 120hr compared to 24hr. In addition, at 24hr, yersiniabactin is detected in greater abundance within the *E. coli* samples than the *E. faecalis* samples, highlighting the capacity for molecular diffusion away from *E. coli* and into the surrounding environment. Single species controls for *E. coli* and *E. faecalis* remain unchanged over time for yersiniabactin. **Figure S3C** shows the constitutive presence of L-ornithine (C00077) in all of the samples, supporting the model for *E. faecalis* contribution of L-ornithine flux in the biofilm, and validating the absence of transcriptional expression changes for OG1RF_10103 encoding *arcD* when in proximity to *E. coli*. In addition to L-ornithine, metabolites central to the arginine biosynthesis pathway including N-acetyl-L-glutamate (C00624), N-acetylornithine (C00437), and L-aspartate (C00049) (**Figure 6A**) were detected in all samples supporting the role of this pathway in *E. faecalis* biofilm and signal exchange with *E. coli*. Overall, this work shows how *E. faecalis* alters the local environment to drive polymicrobial colonization to infection by overcoming local host nutritional immunity.

Discussion

Chronic polymicrobial biofilm-associated infections are prevalent in hospital settings and are difficult to treat due to their increased tolerance to antimicrobial chemotherapeutics. However, the pathogenesis of most polymicrobial interactions remain mechanistically uncharacterized. *E. coli* is a primary cause of UTI, CAUTI, and common in wound infections. *E. coli* is frequently co-isolated with *E. faecalis*; a bacterium also associated with UTI, CAUTI, and wound infections. *E. coli* is a model organism for extensive functional iron acquisition studies, highlighting the importance of these virulence factors in pathogenicity (Neilands, 1993, Neilands, 1995, Skaar, 2010). Our findings demonstrate that *E. faecalis* is a major influence on *E. coli* growth in biofilm when *E. coli* numbers are initially low and experiencing iron limitation. The selectivity of biofilm, and not planktonic culture, for this phenotype is suggestive of cell-to-cell interaction and metabolic cooperation that are fundamental hallmarks of the bacterial biofilm state (Costerton, 1995). Our data support a model of polymicrobial infection in which export of L-ornithine from *E. faecalis* provides a cue for heightened *E. coli* enterobactin induction which allows it to overcome iron limitation and growth restriction (**Fig 6B**). *E. coli* then proliferates to high titers and increases production of virulence-associated siderophores yersiniabactin and salmochelin to further acquire host-restricted iron sources.

Siderophore biosynthesis and chelation efficiency are important factors influencing the strength of the *E. coli* response to iron limitation. *E. coli* UTI89 encodes the catecholate type siderophores enterobactin and salmochelin, and the phenolate type siderophore yersiniabactin (Henderson et al., 2009). The ferric uptake regulator (*fur*) globally derepresses biosynthesis of siderophore genes upon iron limitation in *E. coli* (Huja et al., 2014, Oh et al., 1999). While *E. coli* upregulate siderophore genes under iron-limited conditions in the absence of *E. faecalis*, our data suggest that *E. faecalis* L-ornithine further stimulates enterobactin biosynthesis independent of *fur*. Another example of *fur*-independent transcriptional regulation of a siderophore acquisition system occurs when ferric

citrate binds to the outer membrane receptor FecA in *E. coli*, *P. aeruginosa*, *Klebsiella pneumonia* and other Gram-negative bacteria. This interaction activates the FecI sigma factor and FecR cytoplasmic membrane transducer to increase expression of the *fecABCDE* system (Noinaj et al., 2010, Mahren et al., 2005). Since pH strongly influences chelation efficiency, growth at lower pH ranges and the interaction with the lactic acid bacterium *E. faecalis* may further influence differential thermodynamic efficiency of iron-siderophore binding (Miethke and Marahiel, 2007). In *E. coli* Nissle 1917, a strain which produces four siderophores, yersiniabactin biosynthesis functions optimally at neutral to alkaline conditions (Valdebenito et al., 2006). In contrast, catecholate siderophores such as enterobactin optimally chelate iron at neutral pH but are more efficient than carboxylate siderophores above pH5.0 (Miethke and Marahiel, 2007). We propose that early during *E. faecalis*-*E. coli* interactions, when iron is limited and *E. faecalis* may have a growth advantage, *E. faecalis* lactic acid production favors enterobactin induction in *E. coli*. During later stages of biofilm development, when the local environment becomes alkaline due to *E. coli* metabolic byproduct accumulation, a switch to yersiniabactin would make iron chelation efficiency more favorable.

The arginine deaminase system (ADS) is significant for the generation of ATP and ammonia in many bacteria and is important for biofilm formation in *Staphylococci* (Lindgren et al., 2014). *Streptococcus gordonii* metabolic exchange of ornithine with the oral pathogen *Fusobacterium nucleatum* through the antiporter ArcD has been shown to support *F. nucleatum* biofilm development in mixed species; although, the ornithine-mediated mechanisms that *F. nucleatum* utilizes have not been elucidated (Sakanaka et al., 2015). A homologous *E. faecalis* arginine deaminase pathway is encoded by the *arcABC* genes and the *arcD* antiporter (Barcelona-Andres et al., 2002). Our work demonstrates that mutation of *arcD* in *E. faecalis* disrupts *E. coli* biofilm growth enhancement under iron limitation, while supplementation of ornithine to single species *E. coli* biofilm augments growth for wild type in an enterobactin-dependent manner. Ornithine is a precursor component for the biosynthesis of hydroxamate siderophores; however *E. coli* UTI89 produces only the catecholates enterobactin and salmochelin, and the phenolate yersiniabactin which do not require ornithine as a building block

(Yuan et al., 2001). Ornithine is essential within the *E. coli* arginine biosynthesis pathway which is interconnected with several other biosynthesis and degradative pathways such as pyrimidine and polyamine biosynthesis (Caldara et al., 2006). Metabolomic detection of N-acetyl-L-glutamate (C00624), N-acetylornithine (C00437), and L-aspartate (C00049) in addition to L-ornithine (C00077) confirmed the activity of the arginine biosynthesis pathway. These metabolites are detected in all samples highlighting their importance in cellular metabolism. Differential detection of these by non-targeted LCMS may not be as practical as for the highly biosynthesized siderophores. This pathway is under transcriptional repression control by *argR*, which in the presence of L-arginine accumulation causes feedback inhibition of the pathway via *argA*. This feedback inhibition of N-acetylglutamate synthase causes an increase in aromatic amino acid precursors and has been suggested to link to enterobactin siderophore production (Charlier and Glansdorff, 2004), which may explain *E. faecalis* ornithine driven induction of *E. coli* siderophore biosynthesis during mixed species biofilms. One component of this pathway, *argF*, responds to Fe^{2+}-Fur activation and our data shows decreased transcriptional expression of *argF* when proximal to *E. faecalis* supporting the interpretation that *E. coli* is experiencing iron limitation (Seo et al., 2014). While genes coding for the arginine biosynthesis pathway (*argC*, *argI*, *argE* and *argT*) and the majority of the *E. coli* Fur regulon show increased gene expression, the decrease in *argF* expression may explain a connection between *E. coli* sensing of environmental iron and ornithine. This finding raises the possibility of ornithine targeting as a means of managing biofilm-associated wound infections which are inherently tolerant to antibiotics and are difficult to resolve.

Wound infections are common, often difficult to eradicate, and managed clinically by a combination of broad-spectrum antibiotics, surgical debridement, or amputation. Our work highlights that the diversity of bacterial species in the infection niche is important and that commensal species can have significant influence on the growth, proliferation, and virulence of other pathogens. The deeper understanding of the mechanisms of polymicrobial interactions within wounds that we demonstrate

raises the specter of new approaches for eradicating these recalcitrant, antibiotic-tolerant, biofilm-associated infections.

Experimental Procedures

Bacterial Strains and Growth Conditions. Strains used in this study are listed in **Table S1**. Bacterial growth conditions and *E. coli* mutant generation is detailed in **Supplemental Experimental Procedures**.

Macrocolony Assay. Macrocolonies were inoculated with 1-2x10^6 CFU in a total volume of 5µl. At time points indicated, macrocolonies were excised and resuspended in PBS for enumeration, with n=3 biological experiments for all assays. Macrocolonies were subjected to CFU enumeration by plating on selective media, RNA extraction and sequencing, or metabolite extraction as described in the **Supplemental Experimental Procedures**.

Biofilm Assay. Biofilm assays were initiated by inoculating to 1.6-3.2x10^6 CFU/200µl microtiter well with either single species or mixed species inocula, 200µl aliquoted per well of a 96-well flat bottom transparent microtiter plate (Thermo Scientific, Waltman, MA, USA) and incubated at 37^{o}C under static conditions. Supernatants were discarded and the remaining biofilm stained with crystal violet as described in **Supplemental Experimental Procedures**. Transposon screening performed using this biofilm assay are also detailed in **Supplemental Experimental Procedures**.

Mouse Model of Wound Infection. Bacterial cultures, prepared as described above, were used to infect wounds in 7-week old female C57BL/6J mice (InVivos Pte. Ltd., Lim Chu Kang, Singapore) as described in **Supplemental Experimental Procedures**. All studies and protocols were approved by the Nanyang Technological University Institutional Care and Use Committee (IACUC NTU).

Author Contributions

D.K. and K.A.K. designed experiments, analyzed data, and prepared the manuscript. D.K., W.H.T, and Y.Y.H. performed experiments and analyzed data. J.D. and G.D. provided the transposon library. S.U. and R.B.H.W. analyzed metabolomics data. S.C. generated *E. coli* mutants. S.L.C. and R.B.H.W. analyzed RNA-seq results. All authors reviewed the manuscript.

Acknowledgments

This work was supported by the National Research Foundation and Ministry of Education Singapore under its Research Centre of Excellence Programme. D.K, W.H.T, Y.Y.H and K.A.K were supported by the National Research Foundation under its Singapore NRF Fellowship programme (NRF-NRFF2011-11), and by the Ministry of Education Singapore under its Tier 2 programme (MOE2014-T2-2-124). S.C. and S.L.C. were supported by NRF-RF2010-10. We thank Daniela Moses and colleagues for performing library preparation and RNA sequencing; Sanjay Swarup, Victor Nesati and colleagues for conducting the metabolomics survey; Jeff Henderson and Scott Hultgren for providing *E. coli* siderophore mutants; and Kenneth Beckman and colleagues for sequencing of the *E. faecalis* transposon library.

References

Archibald, F. 1986. Manganese: its acquisition by and function in the lactic acid bacteria. Crit Rev Microbiol, *13*, 63-109.

Barcelona-Andres, B., Marina, A. & Rubio, V. 2002. Gene Structure, Organization, Expression, and Potential Regulatory Mechanisms of Arginine Catabolism in *Enterococcus faecalis*. Journal of Bacteriology, *184*, 6289-6300.

Bourgogne, A., Hilsenbeck, S. G., Dunny, G. M. & Murray, B. E. 2006. Comparison of OG1RF and an isogenic *fsrB* deletion mutant by transcriptional analysis: the *Fsr* system of *Enterococcus faecalis* is more than the activator of gelatinase and serine protease. J Bacteriol, *188*, 2875-84.

Bowler, P. G., Duerden, B. I. & Armstrong, D. G. 2001. Wound microbiology and associated approaches to wound management. Clin Microbiol Rev, *14*, 244-69.

Browne, A. C., Vearncombe, M. & Sibbald, R. G. 2001. High bacterial load in asymptomatic diabetic patients with neurotrophic ulcers retards wound healing after application of Dermagraft. Ostomy Wound Manage, *47*, 44-9.

Bruyneel, B., Vandewoestyne, M. & Verstraete, W. 1989. Lactic-Acid Bacteria - Microorganisms able to grow in the absence of available iron and copper. Biotechnology Letters*, 11*, 401-406.

Budzikiewicz, H. 2010. Microbial siderophores. Fortschr Chem Org Naturst*, 92*, 1-75.

Caldara, M., Charlier, D. & Cunin, R. 2006. The arginine regulon of *Escherichia coli*: whole-system transcriptome analysis discovers new genes and provides an integrated view of arginine regulation. Microbiology, *152*, 3343-54.

Cao, J., Woodhall, M. R., Alvarez, J., Cartron, M. L. & Andrews, S. C. 2007. EfeUOB (YcdNOB) is a tripartite, acid-induced and CpxAR-regulated, low-pH Fe2+ transporter that is cryptic in *Escherichia coli* K-12 but functional in *E. coli* O157:H7. Mol Microbiol*, 65*, 857-75.

Charlier, D. & Glansdorff, N. 2004. Biosynthesis of Arginine and Polyamines. Ecosal Plus*,* 1.

Chaturvedi, K. S., Hung, C. S., Crowley, J. R., Stapleton, A. E. & Henderson, J. P. 2012. The siderophore yersiniabactin binds copper to protect pathogens during infection. Nat Chem Biol*, 8*, 731-6.

Citron, D. M., Goldstein, E. J., Merriam, C. V., Lipsky, B. A. & Abramson, M. A. 2007. Bacteriology of moderate-to-severe diabetic foot infections and in vitro activity of antimicrobial agents. J Clin Microbiol*, 45*, 2819-28.

Costerton, J. W., Lewandowski, Z., Caldwell, D. E., Korber, D. R., & Lappin-Scott, H. M. 1995. Microbial biofilms. Annual Review of Microbiology, 49, 711-45.

Dalton, T., Dowd, S. E., Wolcott, R. D., Sun, Y., Watters, C., Griswold, J. A. & Rumbaugh, K. P. 2011. An in vivo polymicrobial biofilm wound infection model to study interspecies interactions. PLoS One*, 6*, e27317.

Dowd, S. E., Sun, Y., Secor, P. R., Rhoads, D. D., Wolcott, B. M., James, G. A. & Wolcott, R. D. 2008. Survey of bacterial diversity in chronic wounds using pyrosequencing, DGGE, and full ribosome shotgun sequencing. BMC Microbiol*, 8*, 43.

Dunny, G. M., Brown, B. L. & Clewell, D. B. 1978. Induced cell aggregation and mating in *Streptococcus faecalis*: evidence for a bacterial sex pheromone. Proc Natl Acad Sci U S A*, 75*, 3479-83.

Flores-mireles, A. L., Walker, J. N., Caparon, M. & Hultgren, S. J. 2015. Urinary tract infections: epidemiology, mechanisms of infection and treatment options. Nat Rev Microbiol.

Ganz, T. & Nemeth, E. 2012. Hepcidin and iron homeostasis. Biochim Biophys Acta*, 1823*, 1434-43.

Gao, P., Pinkston, K. L., Nallapareddy, S. R., Van Hoof, A., Murray, B. E. & Harvey, B. R. 2010. *Enterococcus faecalis rnjB* is required for pilin gene expression and biofilm formation. J Bacteriol*, 192*, 5489-98.

Garcia, E. C., Brumbaugh, A. R. & Mobley, H. L. 2011. Redundancy and specificity of *Escherichia coli* iron acquisition systems during urinary tract infection. Infect Immun*, 79*, 1225-35.

Giacometti, A., Cirioni, O., Schimizzi, A. M., Del Prete, M. S., Barchiesi, F., D'Errico, M. M., Petrelli, E. & Scalise, G. 2000. Epidemiology and microbiology of surgical wound infections. J Clin Microbiol*, 38*, 918-22.

Gjodsbol, K., Christensen, J. J., Karlsmark, T., Jorgensen, B., Klein, B. M. & Krogfelt, K. A. 2006. Multiple bacterial species reside in chronic wounds: a longitudinal study. Int Wound J*, 3***,** 225-31.
Hancock, L. E. & Perego, M. 2004. The *Enterococcus faecalis fsr* two-component system controls biofilm development through production of gelatinase. J Bacteriol*, 186***,** 5629-39.
Hancock, V., Ferrieres, L. & Klemm, P. 2008. The ferric yersiniabactin uptake receptor FyuA is required for efficient biofilm formation by urinary tract infectious *Escherichia coli* in human urine. Microbiology*, 154***,** 167-75.
Hantke, K., Nicholson, G., Rabsch, W. & Winkelmann, G. 2003. Salmochelins, siderophores of Salmonella enterica and uropathogenic *Escherichia coli* strains, are recognized by the outer membrane receptor IroN. Proc Natl Acad Sci U S A, *100***,** 3677-82.
Henderson, J. P., Crowley, J. R., Pinkner, J. S., Walker, J. N., Tsukayama, P., Stamm, W. E., Hooton, T. M. & Hultgren, S. J. 2009. Quantitative metabolomics reveals an epigenetic blueprint for iron acquisition in uropathogenic *Escherichia coli.* PLoS pathogens*, 5***,** e1000305.
Huja, S., Oren, Y., Biran, D., Meyer, S., Dobrindt, U., Bernhard, J., Becher, D., Hecker, M., Sorek, R. & Ron, E. Z. 2014. Fur is the master regulator of the extraintestinal pathogenic *Escherichia coli* response to serum. MBio*,* 5.
Imbert, M. & Blondeau, R. 1998. On the iron requirement of *lactobacilli* grown in chemically defined medium. Curr Microbiol*, 37***,** 64-6.
Kanehisa, M., Goto, S., Furumichi, M., Tanabe, M. & Hirakawa, M. 2010. KEGG for representation and analysis of molecular networks involving diseases and drugs. Nucleic Acids Res*, 38***,** D355-60.
Kanehisa, M., Goto, S., Sato, Y., Kawashima, M., Furumichi, M. & Tanabe, M. 2014. Data, information, knowledge and principle: back to metabolism in KEGG. Nucleic Acids Res*, 42***,** D199-205.
Klevens, R. M., Edwards, J. R., Richards, C. L., JR., Horan, T. C., Gaynes, R. P., Pollock, D. A. & Cardo, D. M. 2007. Estimating health care-associated infections and deaths in U.S. hospitals, 2002. Public Health Rep*, 122***,** 160-6.
Kristich, C. J., Nguyen, V. T., LE, T., Barnes, A. M., Grindle, S. & Dunny, G. M. 2008. Development and use of an efficient system for random mariner transposon mutagenesis to identify novel genetic determinants of biofilm formation in the core *Enterococcus faecalis* genome. Appl Environ Microbiol*, 74***,** 3377-86.
Lebreton, F., Willems, R. J. L. & Gilmore, M. S. 2014. Enterococcus Diversity, Origins in Nature, and Gut Colonization. *In:* Gilmore, M. S., Clewell, D. B., Ike, Y. & Shankar, N. (eds.) *Enterococci: From Commensals to Leading Causes of Drug Resistant Infection.* Boston.
Lindgren, J. K., Thomas, V. C., Olson, M. E., Chaudhari, S. S., Nuxoll, A. S., Schaeffer, C. R., Lindgren, K. E., Jones, J., Zimmerman, M. C., Dunman, P. M., Bayles, K. W. & Fey, P. D. 2014. Arginine deiminase in *Staphylococcus epidermidis* functions to augment biofilm maturation through pH homeostasis. J Bacteriol, *196***,** 2277-89.
Lisiecki, P. & Mikucki, J. 2004. [Citric acid as a siderophore of *enterococci*?]. Med Dosw Mikrobiol*, 56***,** 29-40.
Lisiecki, P. & Mikucki, J. 2006. Iron supply of *enterococci* by 2-oxoacids and hydroxyacids. Pol J Microbiol*, 55***,** 195-202.
Lv, H. & Henderson, J. P. 2011. Yersinia high pathogenicity island genes modify the *Escherichia coli* primary metabolome independently of siderophore production. J Proteome Res*, 10***,** 5547-54.
Lv, H., Hung, C. S. & Henderson, J. P. 2014. Metabolomic analysis of siderophore cheater mutants reveals metabolic costs of expression in uropathogenic *Escherichia coli.* J Proteome Res*, 13***,** 1397-404.
Magill, S. S., Edwards, J. R., Bamberg, W., Beldavs, Z. G., Dumyati, G., Kainer, M. A., Lynfield, R., Maloney, M., Mcallister-Hollod, L., Nadle, J., Ray, S. M., Thompson, D. L., Wilson, L. E., Fridkin, S. K., Emerging infections program healthcare-associated, I. & antimicrobial use prevalence survey, T. 2014. Multistate point-prevalence survey of health care-associated infections. N Engl J Med*, 370***,** 1198-208.

Mahren, S., Schnell, H. & Braun, V. 2005. Occurrence and regulation of the ferric citrate transport system in *Escherichia coli* B, *Klebsiella pneumoniae*, *Enterobacter aerogenes*, and *Photorhabdus luminescens*. Arch Microbiol*, 184***,** 175-86.
Maki, D. G. & Tambyah, P. A. 2001. Engineering out the risk for infection with urinary catheters. Emerging infectious diseases*, 7***,** 342-7.
Marcelis, J. H., Den Daas-Slagt, H. J. & Hoogkamp-Korstanje, J. A. 1978. Iron requirement and chelator production of *staphylococci*, *Streptococcus faecalis* and *enterobacteriaceae*. Antonie van Leeuwenhoek*, 44***,** 257-67.
Miethke, M. & Marahiel, M. A. 2007. Siderophore-based iron acquisition and pathogen control. Microbiol Mol Biol Rev*, 71***,** 413-51.
Miethke, M., Monteferrante, C. G., Marahiel, M. A. & Van Dijl, J. M. 2013. The *Bacillus subtilis* EfeUOB transporter is essential for high-affinity acquisition of ferrous and ferric iron. Biochim Biophys Acta*, 1833***,** 2267-78.
Nakayama, J., Chen, S., Oyama, N., Nishiguchi, K., Azab, E. A., Tanaka, E., Kariyama, R. & Sonomoto, K. 2006. Revised model for *Enterococcus faecalis fsr* quorum-sensing system: the small open reading frame fsrD encodes the gelatinase biosynthesis-activating pheromone propeptide corresponding to staphylococcal agrd. J Bacteriol*, 188***,** 8321-6.
Nallapareddy, S. R., Singh, K. V., Sillanpaa, J., Garsin, D. A., Hook, M., Erlandsen, S. L. & Murray, B. E. 2006. Endocarditis and biofilm-associated pili of *Enterococcus faecalis*. J Clin Invest*, 116***,** 2799-807.
Neilands, J. B. 1993. Siderophores. Arch Biochem Biophys, *302***,** 1-3.
Neilands, J. B. 1995. Siderophores: structure and function of microbial iron transport compounds. J Biol Chem*, 270***,** 26723-6.
Neut, D., Tijdens-Creusen, E. J., Bulstra, S. K., Van Der Mei, H. C. & Busscher, H. J. 2011. Biofilms in chronic diabetic foot ulcers--a study of 2 cases. Acta Orthop*, 82***,** 383-5.
Nielsen, H. V., Flores-Mireles, A. L., Kau, A. L., Kline, K. A., Pinkner, J. S., Neiers, F., Normark, S., Henriques-Normark, B., Caparon, M. G. & Hultgren, S. J. 2013. Pilin and sortase residues critical for endocarditis- and biofilm-associated pilus biogenesis in *Enterococcus faecalis*. J Bacteriol*, 195***,** 4484-95.
Noinaj, N., Guillier, M., Barnard, T. J. & Buchanan, S. K. 2010. TonB-dependent transporters: regulation, structure, and function. Annu Rev Microbiol*, 64***,** 43-60.
O'Toole, G. A. 2011. Microtiter dish biofilm formation assay. J Vis Exp.
Oh, M., Chai, S. H. & Wee, S. 1999. Isolation and identification of Fur binding genes in *Escherichia coli*. Mol Cells*, 9***,** 517-25.
Pao, S. S., Paulsen, I. T. & Saier, M. H., Jr. 1998. Major facilitator superfamily. Microbiol Mol Biol Rev*, 62***,** 1-34.
Pillai, S. K., Sakoulas, G., Eliopoulos, G. M., Moellering, R. C., Jr., Murray, B. E. & Inouye, R. T. 2004. Effects of glucose on fsr-mediated biofilm formation in *Enterococcus faecalis*. J Infect Dis*, 190***,** 967-70.
Raymond, K. N., Dertz, E. A. & Kim, S. S. 2003. Enterobactin: an archetype for microbial iron transport. Proc Natl Acad Sci U S A*, 100***,** 3584-8.
Sakanaka, A., Kuboniwa, M., Takeuchi, H., Hashino, E. & Amano, A. 2015. Arginine-Ornithine Antiporter ArcD Controls Arginine Metabolism and Interspecies Biofilm Development of *Streptococcus gordonii*. J Biol Chem*, 290***,** 21185-98.
Seo, S. W., Kim, D., Latif, H., O'Brien, E. J., Szubin, R. & Palsson, B. O. 2014. Deciphering Fur transcriptional regulatory network highlights its complex role beyond iron metabolism in *Escherichia coli*. Nat Commun, 5, 4910.
Skaar, E. P. 2010. The battle for iron between bacterial pathogens and their vertebrate hosts. PLoS Pathog, *6***,** e1000949.
Valdebenito, M., Crumbliss, A. L., Winkelmann, G. & Hantke, K. 2006. Environmental factors influence the production of enterobactin, salmochelin, aerobactin, and yersiniabactin in *Escherichia coli* strain Nissle 1917. Int J Med Microbiol*, 296***,** 513-20.

Vebo, H. C., Snipen, L., Nes, I. F. & Brede, D. A. 2009. The transcriptome of the nosocomial pathogen *Enterococcus faecalis* V583 reveals adaptive responses to growth in blood. PLoS One*, 4***,** e7660.
Vebo, H. C., Solheim, M., Snipen, L., Nes, I. F. & Brede, D. A. 2010. Comparative genomic analysis of pathogenic and probiotic *Enterococcus faecalis* isolates, and their transcriptional responses to growth in human urine. PLoS One*, 5***,** e12489.
Weinberg, E. D. 1997. The Lactobacillus anomaly: total iron abstinence. Perspect Biol Med*, 40***,** 578-83.
Wiles, T. J., Kulesus, R. R. & Mulvey, M. A. 2008. Origins and virulence mechanisms of uropathogenic *Escherichia coli*. Exp Mol Pathol*, 85***,** 11-9.
Yuan, W. M., Gentil, G. D., Budde, A. D. & Leong, S. A. 2001. Characterization of the *Ustilago maydis sid2* gene, encoding a multidomain peptide synthetase in the ferrichrome biosynthetic gene cluster. J Bacteriol*, 183***,** 4040-51.

Figure Legends

Figure 1. *E. faecalis* promotes *E. coli* biofilm growth under iron limitation. (**A-B**) *E. coli, E. faecalis*, Mix(1_{Ec}:1_{Ef}), Mix(1_{Ec}:4_{Ef}) and Mix(1_{Ec}:19_{Ef}) biofilm growth in 22D supplemented TSBG. (**C**) Supplementation with 50μM $FeCl_3$ restored biomass to iron replete levels. (**A-C**) Representative images of macrocolonies at 120hr; all scale bars represents 1cm. (**D & E**) Time course enumeration of *E. coli* and *E. faecalis*, respectively, from macrocolonies with single or mixed inoculums under iron limitation. (**F**) *E. coli, E. faecalis* and Mix(1_{Ec}:19_{Ef}) biofilm biomass in TSBG supplemented with 22D. Biomass is represented by crystal violet absorbance values 595nm. Statistical significance was determined by Two-Way ANOVA with Tukey's test for multiple comparisons, **** P<0.0001. (**G**) Enumeration of planktonic growth at 120hr for *E. coli, E. faecalis* and Mix(1_{Ec}:19_{Ef}) in TSBG with 0.1, 0.2 and 0.7mM 22D. (**D-G**) n = 3 with three technical replicates.

Figure 2. *E. faecalis* proximity causes growth and transcriptome changes in *E. coli*. (**A**) Proximity assay of *E. coli* and *E. faecalis* (120hr) macrocolonies respectively in TSBG supplemented with 22D. Macrocolonies were inoculated at increasing distances apart from one another, 1cm nearest (proximal) and 5cm furthest (distal). Scale bar represents 1cm. Sample sites for proximal and distal samples are indicated by black brackets. (**B**) Enumeration at 24hr and 120hr for *E. coli* and *E. faecalis* at both proximal and distal sites, n = 3 with three technical replicates. (**C**) Statistical enrichment analysis of statistically significant *E. coli* pathways within top 100 & 500 differentially regulated genes (Benjamini-Hochberg adjusted P<0.05). *KEGGid*: pathway identifier used by KEGG; *adjP*: Benjamini-Hochberg corrected P-value; *Ngenes*: number of upregulated genes that are member of the pathway; *EF*: enrichment factor, the quotient of the observed proportion of pathway annotated genes to the expected proportion under the null hypothesis of no association. (**D,E,F**) Transcriptional gene expression profiling of *E. coli* in proximity to *E. faecalis*. Differentially regulated genes and functional categories (≥2-fold change, FDR<0.05) for (**C**) *E. coli*, (**E**) for *E. coli* iron related systems, and (**F**) for *E. faecalis* when grown in close proximity to *E. coli*. The black bar indicates the median

value for each functional category; each circle represents one gene with red color indicating a functional category where the median value represents decreased expression, and green indicating increased expression; n = 3 biological replicates.

Figure 3: *E. coli* enterobactin siderophore mutants do not undergo *E. faecalis*-mediated growth enhancement. Proximity assays of 120hr macrocolonies in TSBG supplemented with 22D with *E. faecalis* and (**A**) *E. coli* UTI89Δ*entB*, (**B**) *E. coli* UTI89Δ*iroA*, (**C**) *E. coli* UTI89Δ*ybtS*, and (**D**) *E. coli* UTI89Δ*entB*Δ*ybtS*.

Figure 4: *E. faecalis* co-infection increases the growth of *E. coli* in a mouse model of wound infection. Mouse wound infection with bacterial burdens determined at 24hpi. The *E. coli* inoculum in single species controls and/or mixed species infections was 2-4x10^2CFU/wound for *E. coli* and 2-4x10^6CFU/wound. (**A**) 24hpi *E. coli* CFU for mono-infected and co-infected wounds. (**B**) 24hpi *E. coli* wild type CFU for co-infected compared to *E. coli* UTI89Δ*entB* co-infected wounds. (**C**) *E. faecalis* CFU at 24hpi from wounds co-infected with *E. coli* wild type or *E. coli* UTI89Δ*entB.* Recovered titers of zero were set to the limit of detection of the assay for statistical analyses and graphical representation in all figures. The horizontal bar represents the median value for each group of mice. N = 3 biological replicates. Statistical significance was determined by the Mann-Whitney test with Dunn's post-test for multiple comparisons, *** P=0.0009. Percentages indicate the proportion of data points falling above 1x10^5CFU/wound for each group.

Figure 5: L-ornithine Supplementation Enhances *E. coli* wild type biofilm but not *E. coli* UTI89Δ*entB* under iron limitation. (**A**) *E. coli* biofilm at 120hr in TSBG supplemented with 22D. (**B**) *E. coli* UTI89Δ*entB* biofilm at 120hr in TSBG supplemented with 22D. In both assays, L-ornithine supplementation is indicated by the black bar with concentration indicated above. Representative data from three independent experiments is shown, where the trend is consistent among all.

Statistical significance of the L-ornithine supplemented samples compared to the non-supplemented *E. coli* control was determined by Two-Way ANOVA with Tukey's test for multiple comparisons, * $P \leq 0.05$, ** $P \leq 0.01$, *** $P \leq 0.001$, **** $P \leq 0.0001$.

Figure 6. Model for *E. faecalis* Modulation of the Polymicrobial Infection Niche. (**A**) Schematic representation of the arginine biosynthesis pathway. Genes encoding the enzymes involved at each step are italicized. Metabolites detected via non-targeted metabolomics are highlighted in green. (**B**) Model of a polymicrobial infection niche where *E. faecalis* (blue) modulates *E. coli* (green) through amino acid flux (ornithine). Siderophore biosynthesis and acquisition are indicated by green arrows. Host iron-bound proteins (from serum and intracellular sources) are highlighted red. The model depicts transition from the initial colonization stage with low *E. coli* titers to proliferation and infection at higher *E. coli* titers.

Table 1. Final Transposon Mutants Identified through the Library Screen.

Gene Name	Gene Locus	Description	Genome Position
arcD	OG1RF_10103	UIT3 family protein, antiporter	116023
bmQ	OG1RF_10187	LIVCS family branched chain amino acid cation symporter	184362
-	OG1RF_10350	Transcriptional regulator	362782
-	OG1RF_10620	ABC superfamily ATP binding cassette transporter, ABC protein	657774
malL	OG1RF_11138	Oligo-1,6-glucosidase	1185608
merR	OG1RF_10308	MerR family transcriptional regulator	323110

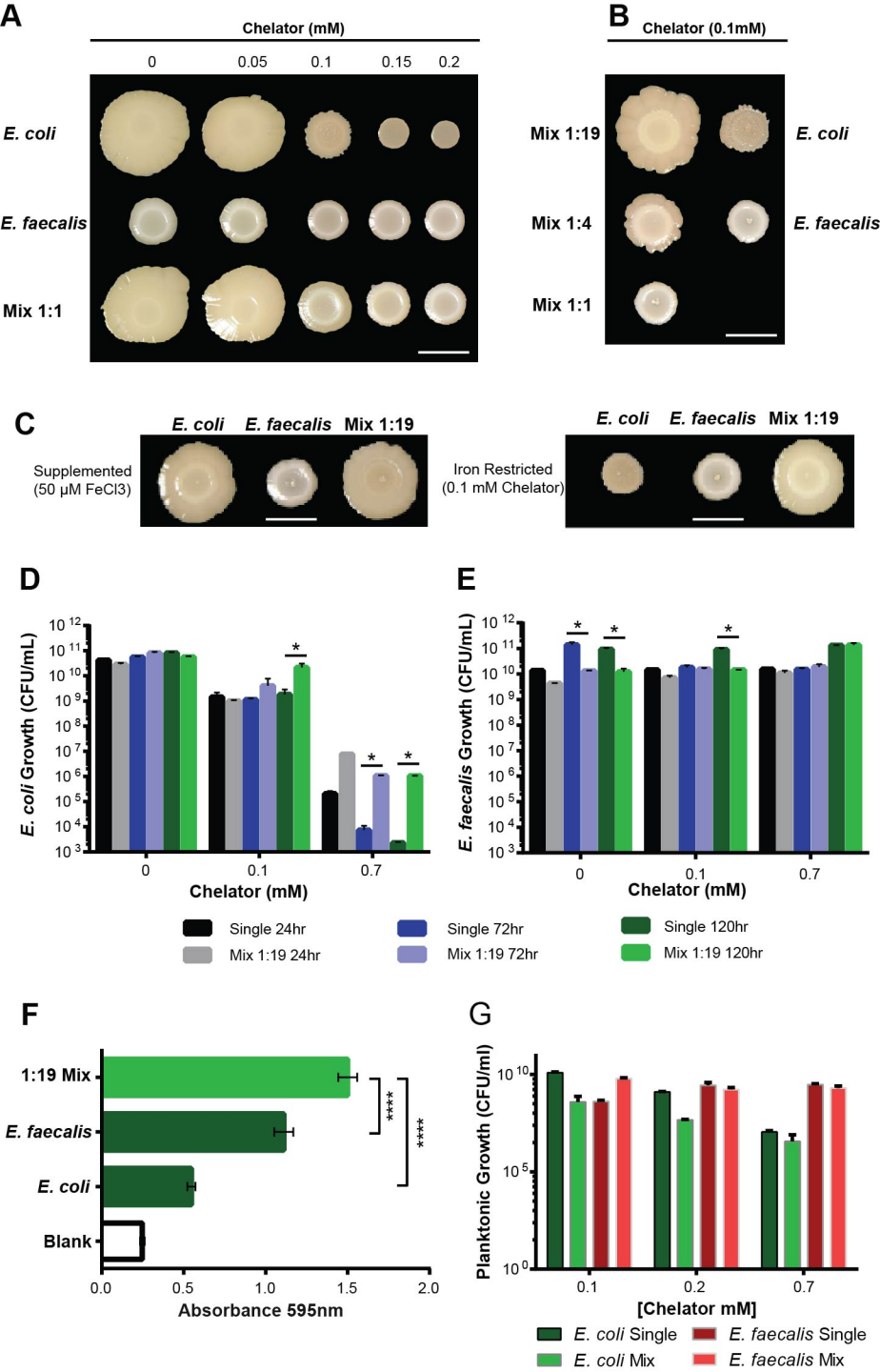
A
Chelator (mM)
0
0.05
0.1
0.15
0.2
E. coli
E. faecalis
Mix 1:1
B
Chelator (0.1mM)
Mix 1:19
Mix 1:4
Mix 1:1
E. coli
E. faecalis
C
E. coli
E. faecalis
Mix 1:19
Supplemented
(50 µM FeCl3)
Iron Restricted
(0.1 mM Chelator)
D
E. coli Growth (CFU/mL)
Chelator (mM)
E
E. faecalis Growth (CFU/mL)
Chelator (mM)
Single 24hr
Mix 1:19 24hr
Single 72hr
Mix 1:19 72hr
Single 120hr
Mix 1:19 120hr
F
1:19 Mix
E. faecalis
E. coli
Blank
****
****
Absorbance 595nm
G
Planktonic Growth (CFU/ml)
[Chelator mM]
E. coli Single
E. coli Mix
E. faecalis Single
E. faecalis Mix

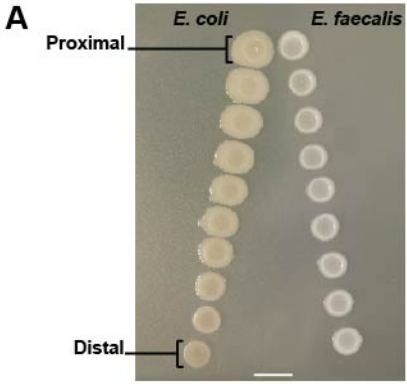

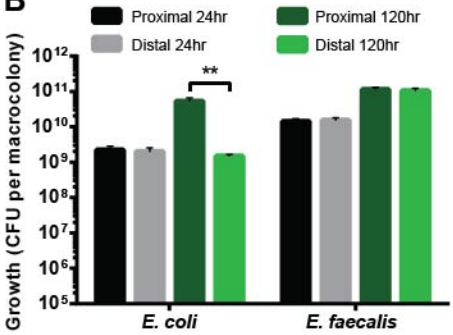

C

Summary of KEGG pathway enrichment analysis across different sets of top ranked upregulated genes

Gene set size		Top 100			Top 500		
Pathway	KEGGid	adjP	Ngenes	EF	adjP	Ngenes	EF
Oxidative phosphorylation	00190	8.7	10	20.6	20.6	26	11.3
Citrate cycle (TCA cycle)	00020	11.8	11	30.0	8.9	15	8.6
Carbon metabolism	01200	10.7	16	11.3	6.3	25	3.7
Biosynthesis of antibiotics	01130	3.5	12	4.9	7.3	36	3.1
Biosynthesis of siderophore group nonribosomal peptides	01053	3.3	4	30.8	7.7	9	14.6
Peptidoglycan biosynthesis	00550	0.0	1	3.8	2.9	8	6.5
Glyoxylate and dicarboxylate metabolism	00630	1.0	4	8.3	1.6	9	3.9
Butanoate metabolism	00650	1.3	4	10.3	0.0	5	2.7
Pyruvate metabolism	00620	0.6	4	6.4	2.0	11	3.7
Fatty acid metabolism	01212	0.0	0	0.0	1.2	6	5.1
Ribosome	03010	0.0	0	0.0	2.5	12	3.9

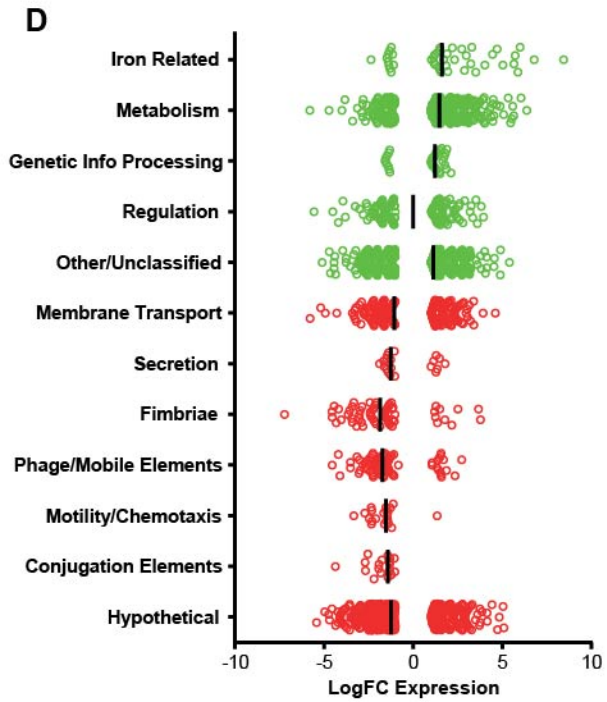

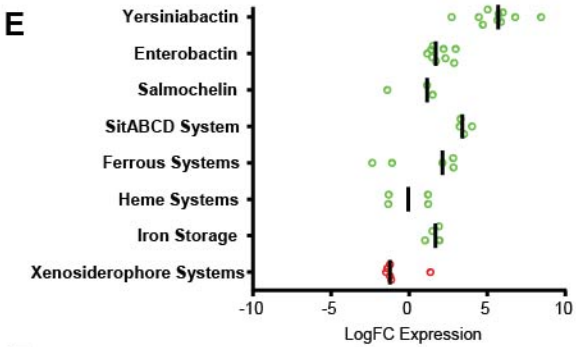

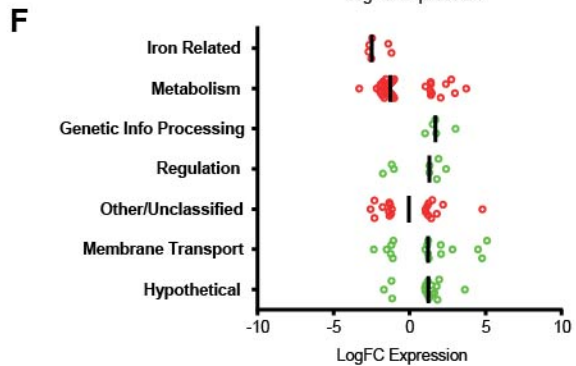

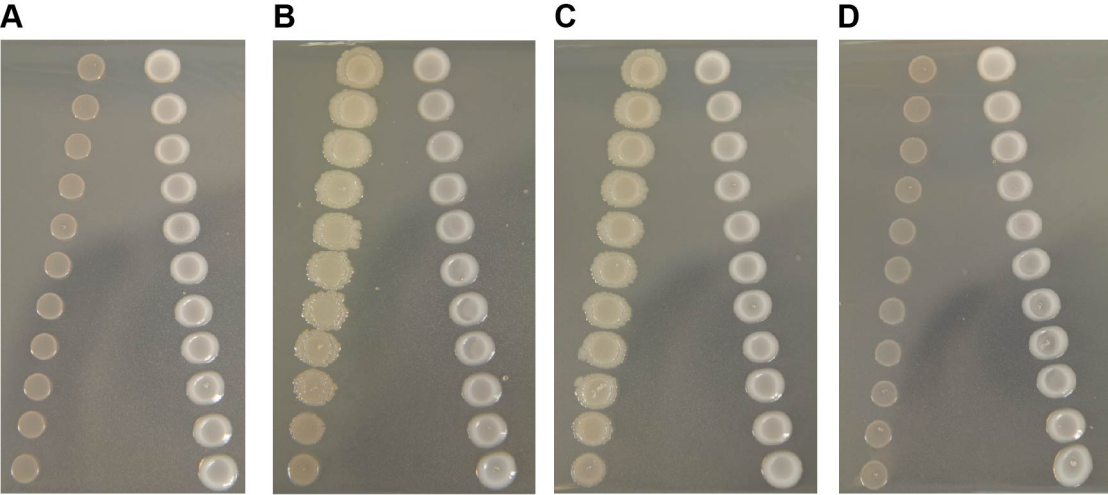
A
B
C
D
E. coli UTI89ΔentB
E. coli UTI89ΔiroA
E. coli UTI89ΔybtS
E. coli UTI89ΔentBΔybtS

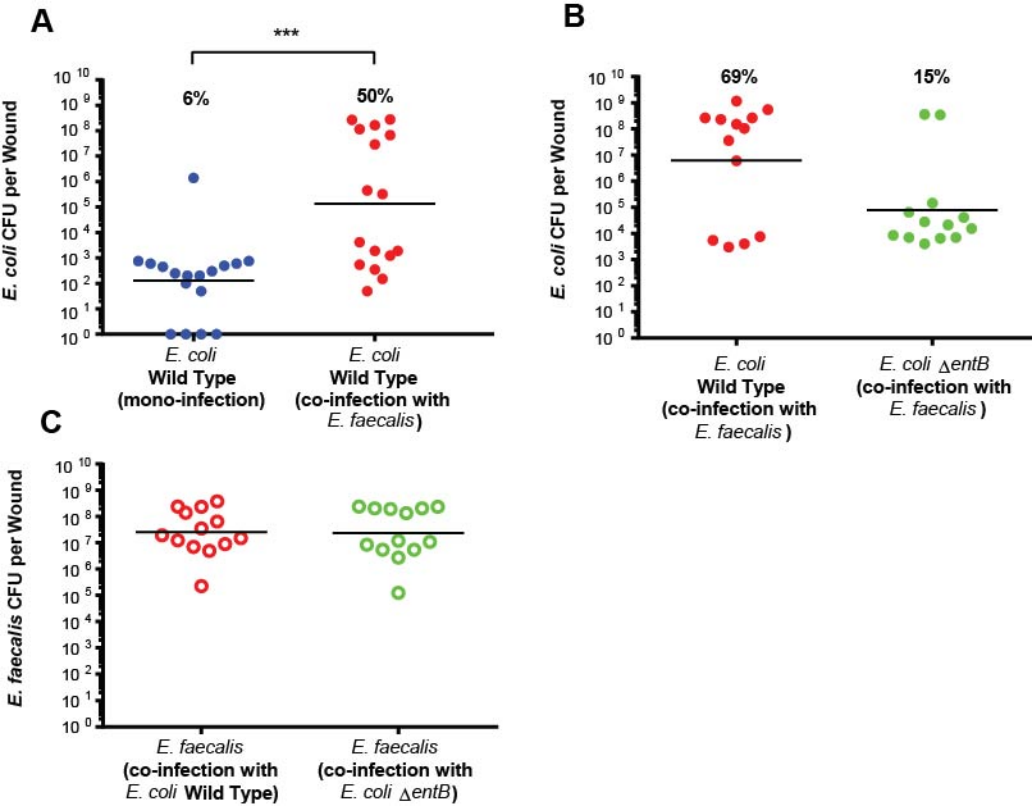
A
***
6%
50%
E. coli CFU per Wound
E. coli
Wild Type
(mono-infection)
E. coli
Wild Type
(co-infection with
E. faecalis)
B
69%
15%
E. coli CFU per Wound
E. coli
Wild Type
(co-infection with
E. faecalis)
E. coli ΔentB
(co-infection with
E. faecalis)
C
E. faecalis CFU per Wound
E. faecalis
(co-infection with
E. coli Wild Type)
E. faecalis
(co-infection with
E. coli ΔentB)

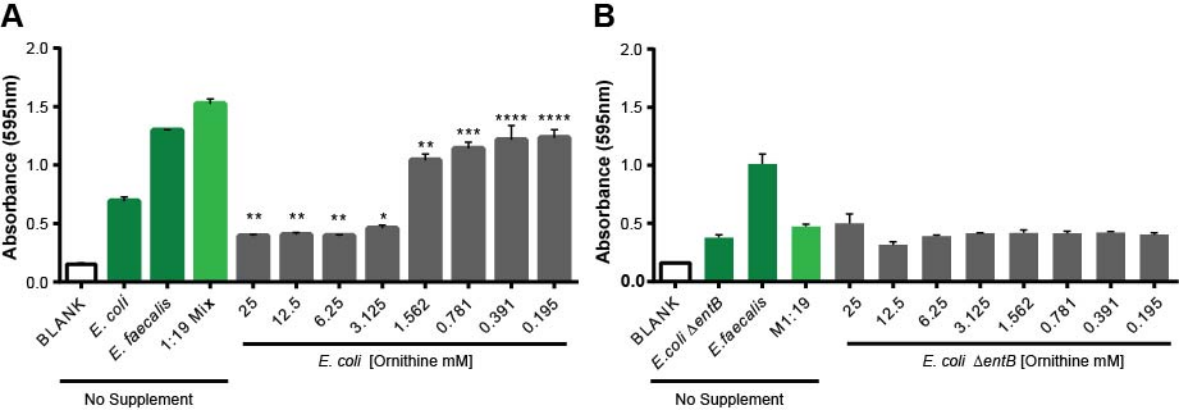
A
Absorbance (595nm)
2.0
1.5
1.0
0.5
0.0
BLANK
E. coli
E. faecalis
1:19 Mix
25
12.5
6.25
3.125
1.562
0.781
0.391
0.195
**
**
**
*
**
***
****
****
E. coli [Ornithine mM]
No Supplement
B
Absorbance (595nm)
2.0
1.5
1.0
0.5
0.0
BLANK
E.coli ΔentB
E.faecalis
M1:19
25
12.5
6.25
3.125
1.562
0.781
0.391
0.195
E. coli ΔentB [Ornithine mM]
No Supplement

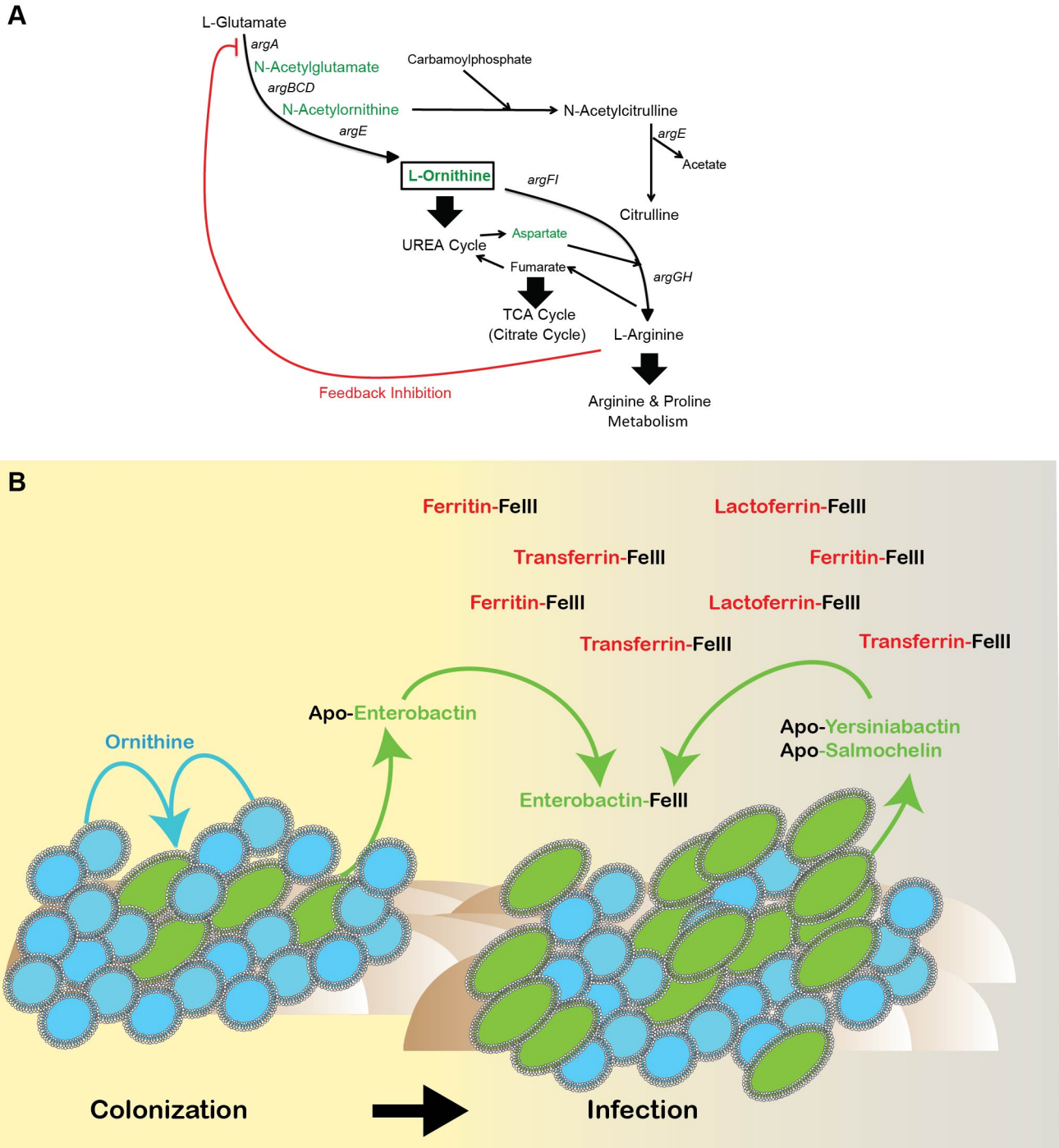
A
L-Glutamate
argA
N-Acetylglutamate
argBCD
N-Acetylornithine
argE
Carbamoylphosphate
N-Acetylcitrulline
argE
Acetate
L-Ornithine
argFI
Citrulline
UREA Cycle
Aspartate
Fumarate
argGH
TCA Cycle
(Citrate Cycle)
L-Arginine
Feedback Inhibition
Arginine & Proline
Metabolism
B
Ferritin-FeIII
Lactoferrin-FeIII
Transferrin-FeIII
Ferritin-FeIII
Ferritin-FeIII
Lactoferrin-FeIII
Transferrin-FeIII
Transferrin-FeIII
Apo-Enterobactin
Ornithine
Apo-Yersiniabactin
Apo-Salmochelin
Enterobactin-FeIII
Colonization
Infection

Supplemental Figures

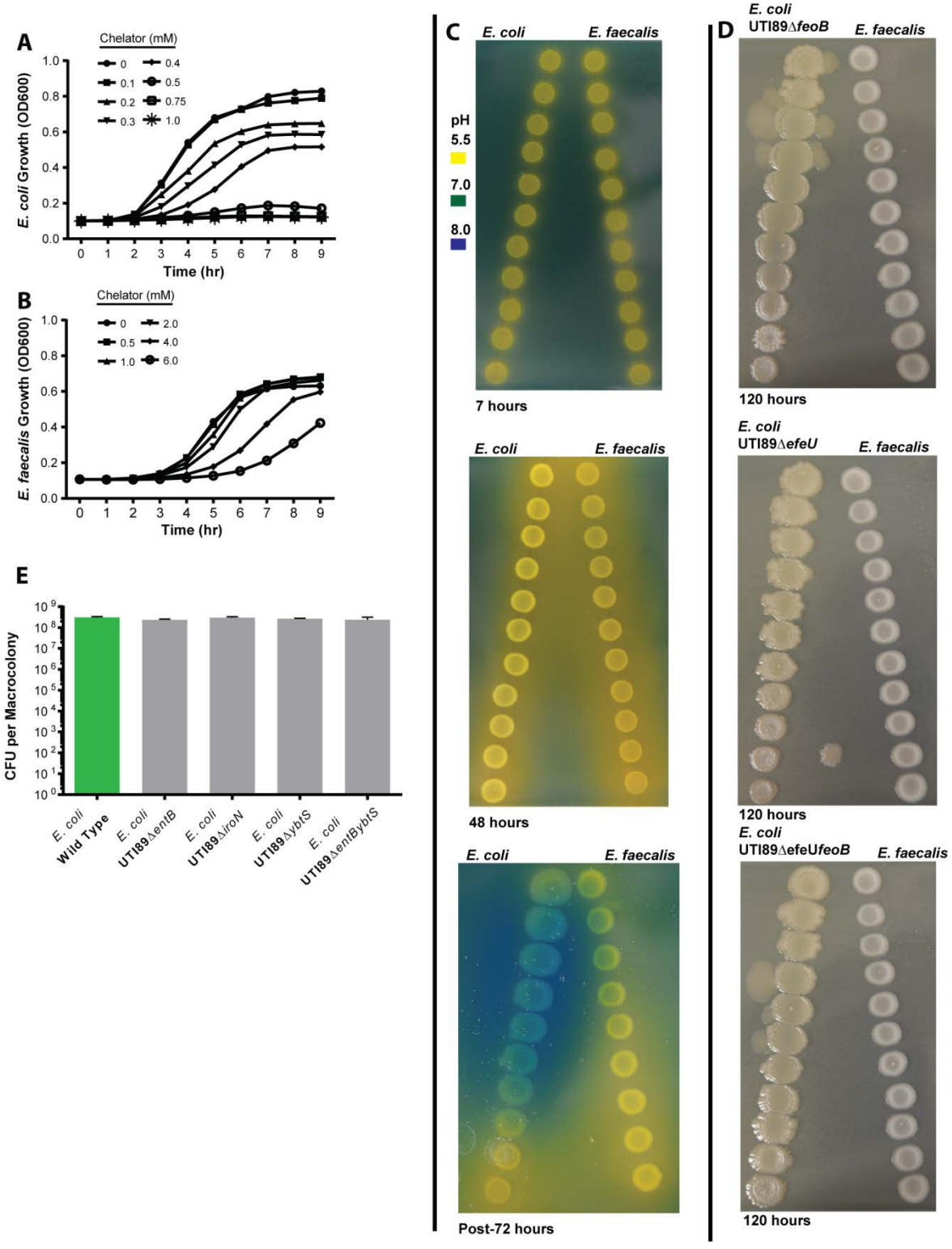

Figure S1. *E. coli* and *E. faecalis* growth responses to iron limitation and proximity (**A & B**) Planktonic growth for *E. coli* and *E. faecalis* respectively in TSBG supplemented with 22D; n = 3, with three technical replicates. (**C**) Proximity assay of *E. coli* and *E. faecalis* macrocolonies in TSBG supplemented with 22D at 7, 48 and 72hr. Bromothymol Blue pH indicator in 1.5% agar solution overlay prior to image capture. (**D**) Proximity assay of *E. coli* ferrous system mutants at 120hr. (**E**) Enumeration of individually cultured *E. coli* siderophore mutant and wild type macrocolonies; n = 3, with three technical replicates.

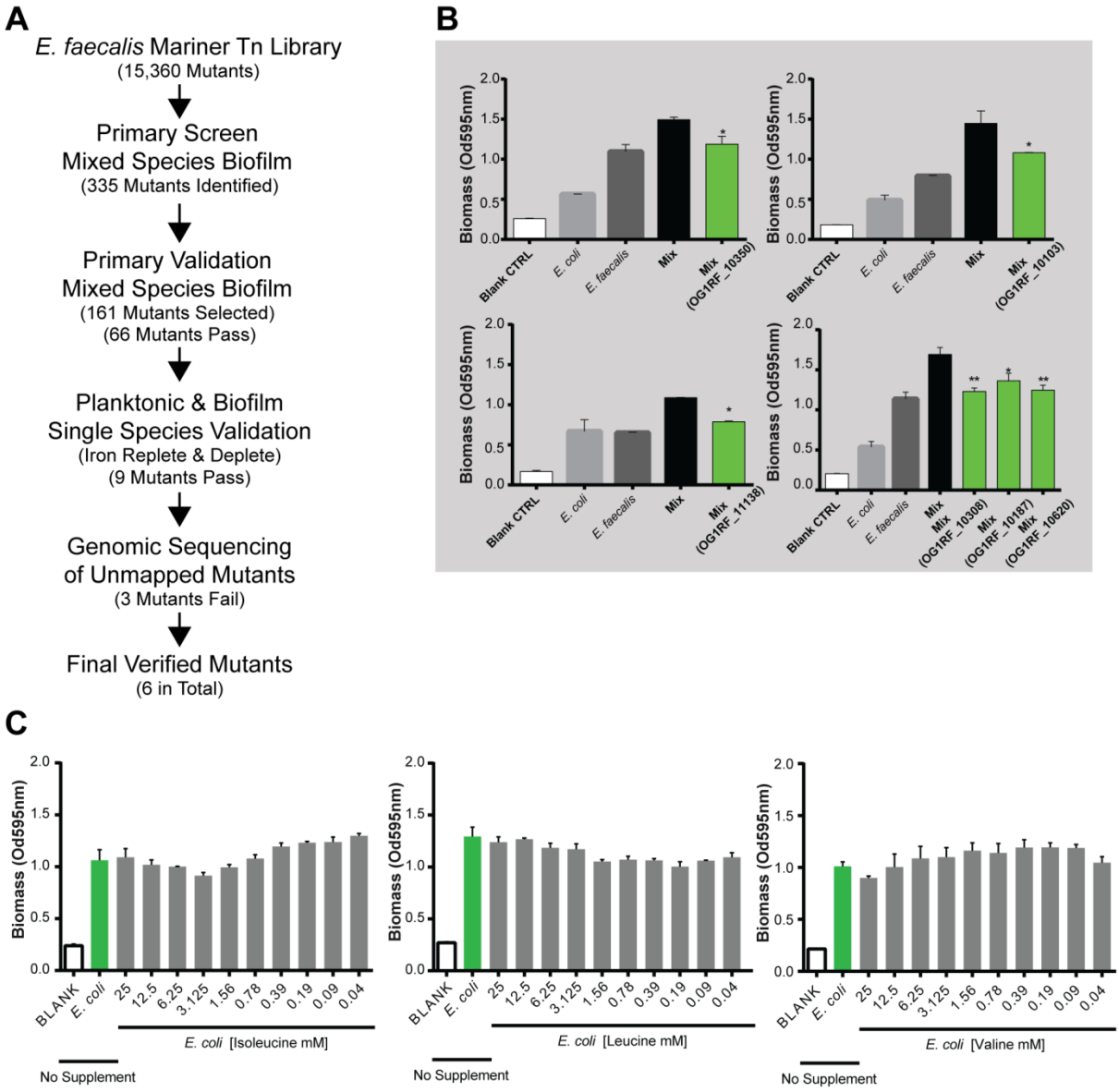

Figure S2. *E. faecalis* transposon library screen and amino acid supplementation (**A**) Workflow of the *E. faecalis* transposon library screen and validation. (**B**) Extracted data from mixed species biofilm validation for final mutants identified through transposon library screening. *E. coli*, *E. faecalis* and Mix(1_{Ec}:19_{Ef}) wild type and transposon mutant biofilm biomass in TSBG supplemented with 22D. Biomass is represented by crystal violet absorbance values 595nm. (**C**) *E. coli* biofilm at 120hr in TSBG supplemented with 22D, and Isoleucine, Leucine, and Valine respectively. Amino acid supplementation is indicated by the black bar with concentration indicated above. Representative data from three independent experiments is shown, where the trend is consistent among all. Statistical significance was determined by Two-Way ANOVA with Tukey's test for multiple comparisons, * $P \leq 0.05$, ** $P \leq 0.01$.

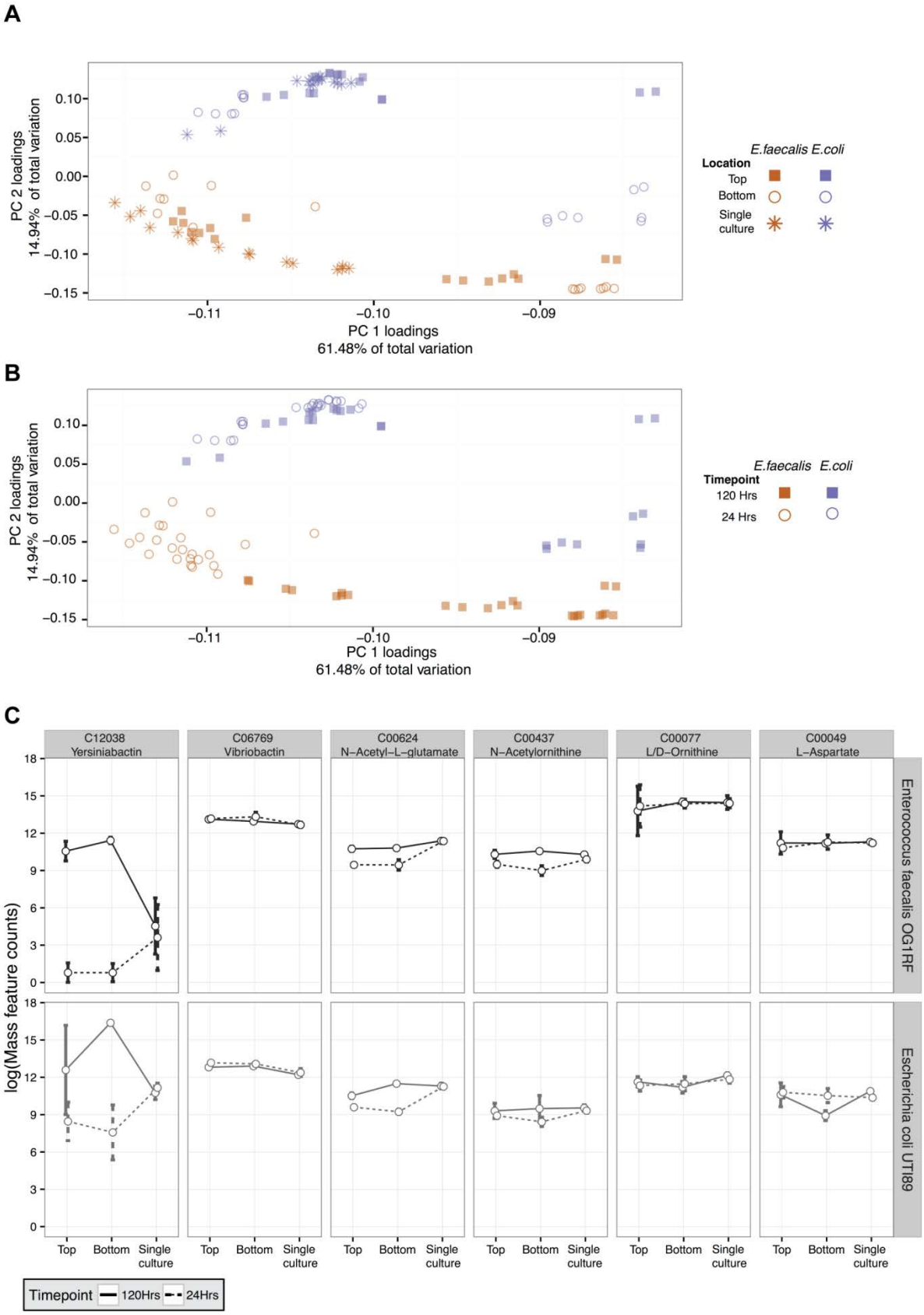

Figure S3. Untargeted metabolic survey of *E. coli* and *E. faecalis* proximity macrocolonies (**A & B**) Analysis of *E. coli* and *E. faecalis* metabolic profiles generated from both single and mixed species macrocolonies at 24 and 120 hours. Log transformed and quantile normalized data is analysed using principal components analysis (PCA). The plane formed by the first two 2 principal component loadings are shown. Each

individual point represents a sample, with its colour indicating the corresponding macrocolony. Panels A and B show identical data, with only the annotations corresponding to the shape of the point being different. (**A**) Filled square and open circles correspond to the location, either top or bottom, of the macrocolonies in the mixed culture experiments, and stars denote samples obtained from a single culture experiments. (**B**) Filled square indicate samples collected at 120 hours, while open circles represent samples collected at 24 hours. (**C**) Mass features have been mapped onto metabolites from KEGG (2015 version) *E. coli* O18:K1:H7 UTI89 (UPEC) and *E. faecalis* OG1RF databases. Mass features were putatively annotated onto metabolites that are within 10 ppm (+- 10 ppm of the mass feature). The first row in the plot shows the trends for Yersiniabactin, Vibriobactin and L/D-Ornithine metabolites from *E. faecalis*, while the second row shows trend for the same metabolites from *E. coli*. X axis indicates the location of the culture, while Y axis indicates the log normalized counts. The line type indicates the time point (growth stage) while the error bars represent the standard deviation calculated from the replicates.

Supplemental Tables

Table S1: List of strains, plasmids, and primers.

Primer Name	Length	Target Position	Sequence	Note
feoB+3792996-P1-FWD	70	3792996	CAAAAAAGATCTGGCCTTATTAGAAGTGGAAGCGGTTTCCTGTTAATACGGTGTAGGCTGGAGCTGCTTC	feoB knockout primer
feoB-3795429-P2-REV	70	-3795429	GTAATGCCAGTAAATCACGCACTTGAATGAGCGAAGCCATTGTCGTGTCCCATATGAATATCCTCCTTAG	feoB knockout primer
feoB -3795656-REV	20	-3795656	GGGCTTTTCAAAACAGGTGA	For colony PCR and sequencing.
feoB +3792597-FWD	21	3792597	GCTGCGATATAACCTTGAGCC	For overlap PCR for clean deletion of feoB, for clony PCR and sequencing
feoB -3793060-REV+20bpL	37	-3793060	ACTTGAATGAGCGAAGCCATTGTTGTTATCACCGTAT	For overlap PCR for clean deletion of feoB
feoB +3795390-FWD+20bpR	37	3795390	ATACGGTGATAACAACAATGGCTTCGCTCATTCAAGT	For overlap PCR for clean deletion of feoB
feoB -3795934-REV	20	-3795934	TGGGTGCCGGTAAATGAAAC	For overlap PCR for clean deletion of feoB
efeU +1067905-P1-FWD	70	1067905	ACTGCGATTTACTTTTCTTTGCATAGATTGACTCAGAAAAACGTTTAAGGGTGTAGGCTGGAGCTGCTTC	efeU knockout primer
efeU -1068844-P2-REV	70	-1068844	CTATCCCTTTAAAGTATGTTGTAACTAAGCAAGAGTTTGCGTCGTATTTGCATATGAATATCCTCCTTAG	efeU knockout primer
efeU+1067485-FWD	20	1067769	CACGTCATAACCGGAAGCAG	For overlap PCR for clean deletion of efeU
efeU -1067963+20bpL-REV	40	-1067963	CGGCGGAAGTTAATGGTCATGCCACCCACCCTTAAACGTT	For overlap PCR for clean deletion of efeU
efeU +1068852+20bpR-FWD	40	1068852	AACGTTTAAGGGTGGGTGGCATGACCATTAACTTCCGCCG	For overlap PCR for clean deletion of efeU
efeU -1069424-REV	20	-1069424	GGAGAACAGTTCAGCAATCGG	For overlap PCR for clean deletion of efeU

efeU +1067785_testFWD	20	1067785	GCAGGCAGAGGGCAATCAGT	For colony PCR and sequencing
efeU-1069005_testREV	20	-1069005	TCCCGGCGTTAACCGTAATG	For colony PCR and sequencing

Plasmid Name	**Description**	**Citation**
pSLC-242	Negative selection cassettes: chlor-prhaB-relE	(Khetrapal et al., 2015)
pSLC-217	negative selection cassettes: kan-prhaB-relE	(Khetrapal et al., 2015)
pKM208	Red-helper plasmid that contains the recombinase, was transformed into the relevant strains for recombination.	(Datsenko and Wanner, 2000)

Strain Name	**Description**	**Citation**
E. coli UTI89	Uropathogenic clinical isolate	(Chen et al., 2006)
E. coli UTI89Δ*entB*	In-frame deletion of *entB*	(Henderson et al., 2009)
E. coli UTI89Δ*iroA*	In-frame deletion of *iroA*	(Lv et al., 2014)
E. coli UTI89Δ*ybtS*	In-frame deletion of *ybtS*	(Henderson et al., 2009)
E. coli UTI89Δ*entB*Δ*ybtS*	In-frame deletion of *entB and ybtS*	(Henderson et al., 2009)
E. coli BW23473	*pri+* for negative selection mutagenesis	
E. coli SLC-554	In-frame deletion of *feoB* in strain UTI89	This Study
E. coli SLC-555	In-frame deletion of *efeU* in strain UTI89	This Study
E. coli SLC-556	In-frame deletion of *feoB* and *efeU* in strain UTI89	This Study
E. faecalis OG1RF	Clinical isolate, ATCC47077	(Dunny et al., 1978)

Supplemental Experimental Procedures

Bacterial Growth Conditions. *Enterococcus faecalis* OG1RF (ATCC47077) (Dunny et al., 1978) was grown in Brain Heart Infusion broth (BHI), *Escherichia coli* UTI89 (Chen et al., 2006) was grown in Luria-Bertani (LB) broth, and both cultured at 37^{o}C under static conditions. When selective media was required, MacConkey agar was used for *E. coli* and BHI supplemented with colistin at 10µg/ml and nalidixic acid at 10µg/ml for *E. faecalis*. BHI, LB, and MacConkey media was supplied by Becton, Dickinson and Company, Franklin Lakes, NJ. TSB medium was supplied by Oxoid Inc., Ontario, Canada. Overnight cultures were normalized to 2-4x10^{8} CFU/ml in phosphate buffered saline (PBS) to OD_{600nm} 0.4 and 0.7 for *E. coli* and *E. faecalis*, respectively, prior to dilution for assays described below. For planktonic and biofilm assays, bacteria were cultured at 37^{o}C under 200rpm or static conditions on tryptone soy broth supplemented with 10mM glucose (TSBG) and solidified with 1.5% Agar when appropriate (Oxoid Technical No.3). Iron depletion was achieved by supplementation with 2,2'dipyridyl (22D) (Sigma Aldrich, St Louis, MO, USA).

Mutagenesis of *E. coli* UTI89. Genes targeted for mutagenesis were deleted in-frame by incorporating a positive-negative selection cassette (*kan*-P_{rhaB}-*relE* or *chlor*-P_{rhaB}-*relE*) from pSLC-217 or pSLC-242, respectively, by Lambda Red-mediated recombination, followed by a second recombination to remove the

cassette with a DNA fragment of the region flanking the gene target, as previously described (Khetrapal et al., 2015). **Table S1** lists the gene targets, primers and corresponding positive-negative selection cassette for each mutagenesis.

Crystal Violet Staining of Biofilm Assays. Microtitre plates were washed twice with PBS. Crystal violet solution 0.1% w/v (Sigma-Aldrich, St Louis, MO, USA) was used to stain surface adherent bacteria by added 200µl/well and incubated at 4°C for 30minutes. This solution was discarded, the microtitre plate washed twice with PBS followed by crystal violet solubilization with 200µl/well ethanol-acetone (4:1) for 45 minutes at room temperature. The intensity of crystal violet staining was measured by absorbance at OD_{595nm} using a Tecan Infinite 200 PRO spectrophotometer (Tecan Group Ltd., Männedorf, Switzerland). n=3 biological replicates with three technical replicates for all biofilm assays.

Transposon Library Screen. An *E. faecalis* OG1RF mariner transposon library containing 14978 mutants was cryogenically stocked in individual 96-well format microtitre plates (Kristich et al., 2008). These were cultured with a cryo-replicator (Adolf Kühner AG) to inoculate 2ml DeepWell blocks (Greiner Bio-One) containing 1ml BHI medium with overnight incubation at 37°C and 220rpm. Cultures were the normalized to an OD_{600nm} of 0.1 (2-4x10^8 CFU/ml) in PBS. *E. coli* culture stocks were normalized to an OD_{600nm} 0.4 to yield 2-4x10^8 CFU/ml in PBS. A primary screen of the *E. faecalis* transposon library was performed by inoculating iron depleted TSBG medium to 8-16x10^4 CFU/200µl microtitre well with *E. coli* and 1.5-3x10^6 CFU/200µl microtitre well of the normalized transposon mutant cultures resulting in an inoculum mix ratio of 1_{Ec}:19_{Ef}. The microtitre plates were then incubated for 120 hours at 37°C statically inside a moistened chamber to prevent evaporation of media. Biofilm was quantified by crystal violet staining as described above and mutants with reduced signal compared to wild type were validated by in the same assay with two independent biological replicates for each mutant. Secondary validations of the transposon mutants were performed to quantify planktonic and biofilm growth profiles of each mutant in single species under iron replete and deplete conditions. Planktonic growth was measured by recording the OD_{600nm} over a period of 14 hours at 37°C with the Tecan Infinite® 200 PRO spectrophotometer (Tecan Group Ltd).

Mapping Tn Insertions

gDNA from transposon mutants not originally mapped were extracted using the Wizard® Genomic DNA Purification Kit (Promega, Madison, WI, USA), quantified and assessed for nucleic acid quality by Qubit High Sensitive dsDNA assay (Invitrogen, Carlsbad, CA, USA) and NanoDrop. Samples were sequenced by Illumina MiSeq, *de novo* reads were assembled using CLC Genomics Workbench version 8.0 and the resultant contigs BLASTed against the mariner transposon used to generate the *E. faecalis* OG1RF Tn Library. Alignment of sequences to the contig identified the insertion site.

RNA extraction, RNAseq and Analysis

Mature macrocolonies cultured for 120hr on iron limited TSBG, in biological triplicate, were subjected to total RNA isolation by bacterial cell disruption with Lysing Matrix D (MP Biomedicals) in TRIzol Reagent (Ambion) for RNA extraction. This was followed by chloroform extraction and isopropanol precipitation to purify the nucleic acids. DNase treatment (TURBO DNA-free kit, Ambion) facilitated removal of contaminating genomic DNA. Measurement of RNA concentration, quality and potential DNA contamination were quantified with Qubit RNA Assay and Qubit High Sensitive dsDNA assay (Invitrogen). Ribosomal RNA (rRNA) was depleted from RNA samples using the Ribo-Zero Magnetic Bacterial Kit (Epidemiology; Epicentre), and the remaining RNA subjected to library preparation for sequencing on an Illumina HiSeq2500 machine. Qubit RNA Assay and Qubit High Sensitive dsDNA assay (Invitrogen) were again used to quantify RNA quality and purity. A minimum concentration of 40-80 ng/µl rRNA depleted RNA, DNA:RNA 1:10 maximum, and a RIN value ≥ 8.0 as measured by Agilent RNA ScreenTape (2200 TapeStation System) were required QC checks prior to Illumina sequencing.

RNA sequencing reads were mapped to the *E. coli* UTI89 reference genome (NCBI accession: NC_007946.1 and NC_0079461.1) or the *E. faecalis* OG1RF reference genome (NCBI accession: NC_017316.1) using BWA (v0.5.9) with default parameters (Li and Durbin, 2009, Nagalakshmi et al., 2010). Sequencing reads (Accession number PRJNA339105) mapping to predicted open reading frames (ORFs) were quantified using HTSeq (Anders et al., 2015). Ribosomal sequences were filtered out of the data set. Differential expression analyses were performed in R (version 2.15.1) using the Bioconductor package, *edgeR* (Robinson et al., 2010). Significantly differentially expressed genes were determined using an FDR cutoff of 0.05 and a fold-change cutoff of 2 (either up- or down-regulated). We annotated differentially expressed genes using a combination of KEGG annotations, as well as manual annotation using operon and other functional data from literature analysis.

To perform pathway enrichment analysis, we sourced the KEGG annotations for all genes in the *E. coli* UTI89 reference genome (KEGG genome identifier: *eci*), contained in the data file *eci_gene_map.tab*. For pathways that contained more than 5 genes detected in this experiment, we constructed 2-by-2 contingency tables by classifying genes based on membership of a pathway and their differential expression status, respectively. The hypothesis of non-random association was tested using Fisher's Exact Test. *P*-values were corrected the number of pathways tested using the Benjamini-Hochberg procedure. Separate analyses were performed for up- and down-regulated genes. The entire analysis was repeated across the following of top ranked genes partitions (*N*=100, 200, 300, 500, 700 and 1000) to gain further insight into the robustness at different false discovery rate thresholds (**Table S2 & S3**).

Model of Mouse Wound Infection. Mice were anesthetized by inhalation of 3% isoflurane and wounds were prepared by shaving a 3x5cm area on the back, sterilization of the skin surface with 70% ethanol, followed by puncturing a single 6mm diameter biopsy through the skin. Following inoculation of bacterial cultures in 5ul PBS, Tegaderm™ dressing (3M, St Paul Minnesota, USA) was applied over the wound. At indicated time points, mice were euthanized and a 144mm^2 area encompassing the wound was excised. The bacteria present in the wound were determined by homogenization and plating of serial dilutions of each sample on selective media. Recovered titers of zero were set to the limit of detection of the assay for statistical analyses and graphical representation in all figures. Statistical significance was determined by the Mann-Whitney test with Dunn's post-test for multiple comparisons with Prism software (version 6 for Windows; GraphPad Software).

Metabolite extraction, LCMS and Analysis

Macrocolony samples, in biological triplicate, from the top (proximal) and bottom (distal) of the proximity assay at both 24hr and 120hr time points were excised and resuspended in 10% MeOH. Cell and agar debris were removed by centrifugation and the supernatant containing the extracted metabolites was collected. Metabolite extracts for four biological replicates of each sample and time point was used for non-targeted metabolite profiling. Each biological replicate was injected twice as analytical replicates. Metabolite profiling was performed using the Acquity UHPLC system (Waters) in-line with LTQ-Orbitrap Velos (Thermo Fisher Scientific). Raw data from Orbitrap (.RAW files) were processed using XCMS (Patti et al., 2012, Smith et al., 2006) in R (R Core Team, 2014). Mass feature abundance matrices were normalized using log10 transformation followed by quantile normalization. Mass features were then mapped (with mass tolerance < 10ppm) onto *E. coli* O18:K1:H7 UTI89 (UPEC) (KEGG genome identifier: eci) and *E. faecalis* OG1RF (KEGG genome identifier: efi) (2015 version) metabolite databases (Kanehisa et al., 2014, Kanehisa and Goto, 2000) using PCDL manager (Agilent).

Supplemental References

Anders, S., Pyl, P. T. & Huber, W. 2015. HTSeq--a Python framework to work with high-throughput sequencing data. Bioinformatics, *31***,** 166-9.

Chen, S. L., Hung, C. S., Xu, J., Reigstad, C. S., Magrini, V., Sabo, A., Blasiar, D., Bieri, T., Meyer, R. R., Ozersky, P., Armstrong, J. R., Fulton, R. S., Latreille, J. P., Spieth, J., Hooton, T. M., Mardis, E. R., Hultgren, S. J. & Gordon, J. I. 2006. Identification of genes subject to positive selection in uropathogenic strains of *Escherichia coli*: a comparative genomics approach. Proceedings of the National Academy of Sciences of the United States of America, *103***,** 5977-82.

Datsenko, K. A. & Wanner, B. L. 2000. One-step inactivation of chromosomal genes in *Escherichia coli* K-12 using PCR products. Proc Natl Acad Sci U S A, *97***,** 6640-5.

Kanehisa, M. & Goto, S. 2000. KEGG: kyoto encyclopedia of genes and genomes. Nucleic Acids Res, *28***,** 27-30.

Khetrapal, V., Mehershahi, K., Rafee, S., Chen, S., Lim, C. L. & Chen, S. L. 2015. A set of powerful negative selection systems for unmodified Enterobacteriaceae. Nucleic Acids Res, *43***,** e83.

Li, H. & Durbin, R. 2009. Fast and accurate short read alignment with Burrows-Wheeler transform. Bioinformatics, *25***,** 1754-60.

Lv, H., Hung, C. S. & Henderson, J. P. 2014. Metabolomic analysis of siderophore cheater mutants reveals metabolic costs of expression in uropathogenic *Escherichia coli*. J Proteome Res, *13***,** 1397-404.

Nagalakshmi, U., Waern, K. & Snyder, M. 2010. RNA-Seq: a method for comprehensive transcriptome analysis. Curr Protoc Mol Biol, Chapter 4**,** Unit 4 11 1-13.

Patti, G., Tautenhahn, R. & Siuzdak, G. 2012. Meta-analysis of untargeted metabolomic data from multiple profiling experiments. Nat. Protoc., *7***,** 508-516.

R CORE TEAM 2014. R: A language and environment for statistical computing. Vienna, Austria: R Foundation for Statistical Computing.

Robinson, M. D., McCarthy, D. J. & Smyth, G. K. 2010. edgeR: a Bioconductor package for differential expression analysis of digital gene expression data. Bioinformatics, *26***,** 139-40.

SMITH, C. A., WANT, E. J., O'MAILLE, G., ABAGYAN, R. & SIUZDAK, G. 2006. XCMS: processing mass spectrometry data for metabolite profiling using nonlinear peak alignment, matching, and identification. *Anal Chem,* 78**,** 779-87.